

การวิเคราะห์ฟิล์มพาสซีฟของเหล็กกล้าไร้สนิมเกรด SUS 304 และ SUS 447J1
ที่ผ่านการทิ้งไว้ในบรรยากาศเขตเมืองอุตสาหกรรม



สถาบันวิทยบริการ
จุฬาลงกรณ์มหาวิทยาลัย

วิทยานิพนธ์นี้เป็นส่วนหนึ่งของการศึกษาตามหลักสูตรปริญญาวิศวกรรมศาสตรมหาบัณฑิต

สาขาวิชาวิศวกรรมโลหการ ภาควิชาวิศวกรรมโลหการ

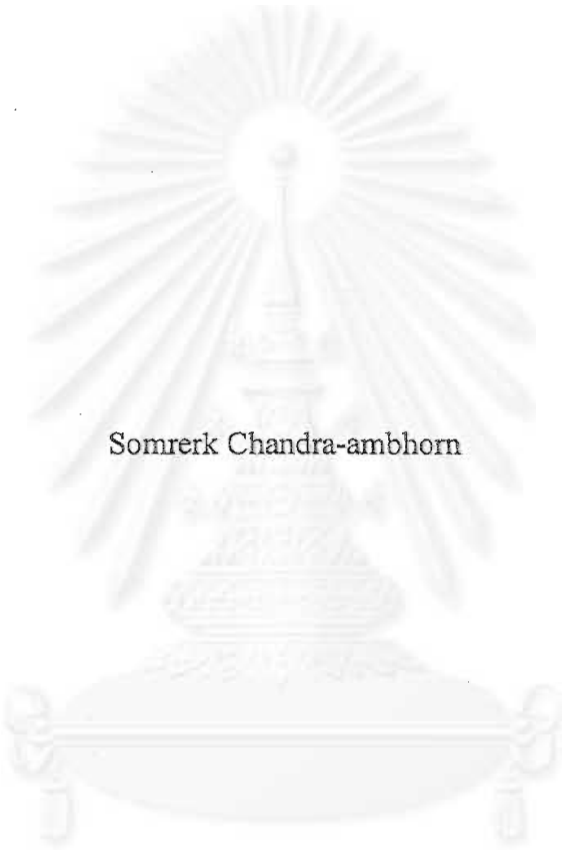
คณะวิศวกรรมศาสตร์ จุฬาลงกรณ์มหาวิทยาลัย

ปีการศึกษา 2544

ISBN 974-03-0318-8

ลิขสิทธิ์ของจุฬาลงกรณ์มหาวิทยาลัย

ANALYSIS OF PASSIVE FILMS FORMED ON SUS 304 AND SUS 447J1
STAINLESS STEEL EXPOSED IN AN URBAN-INDUSTRIAL ATMOSPHERE



Somrek Chandra-ambhorn

สถาบันวิทยบริการ
วไลยอลงกรณ์มหาวิทยาลัย

A Thesis Submitted in the Partial Fulfillment of the Requirements
for the Degree of Master of Engineering in Metallurgical Engineering
Department of Metallurgical Engineering
Faculty of Engineering
Chulalongkorn University
Academic Year 2001
ISBN 974-03-0318-8


Thesis Title Analysis of Passive Films Formed on SUS 304 and SUS 447J1
Stainless Steel Exposed in an Urban-industrial Atmosphere

By Mr. Somrerak Chandra-ambhorn

Field of Study Metallurgical Engineering

Thesis Advisor Assistant Professor Gobboon Lothongkum, Dr.-Ing.

Accepted by the Faculty of Engineering, Chulalongkorn University in the Partial
Fulfillment of the Requirements for the Master's Degree

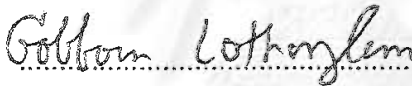
.....Dean of Faculty of Engineering

(Professor Somsak Panyakeow, D.Eng.)

Thesis Committee

.....Chairman

(Associate Professor Prasonk Sricharoenchai, D.Eng.)

.....Thesis Advisor

(Assistant Professor Gobboon Lothongkum, Dr.-Ing.)

.....Member

(Sawai Danchaivijit, Ph.D.)

สถาบันวิทยบริการ
วาลงกรณ์มหาวิทยาลัย

สมฤกษ์ จันทรอัมพร: การวิเคราะห์ฟิล์มพาสซีฟของเหล็กกล้าไร้สนิมเกรด SUS 304 และ SUS 447J1 ที่ผ่านการทิ้งไว้ในบรรยากาศเขตเมืองอุตสาหกรรม. (ANALYSIS OF PASSIVE FILMS FORMED ON SUS 304 AND SUS 447J1 STAINLESS STEEL EXPOSED IN AN URBAN-INDUSTRIAL ATMOSPHERE)

อ.ที่ปรึกษา: ผศ.ดร.กอบบุญ หล่อทองคำ, 43 หน้า. ISBN 974-03-0318-8.

การทดลองในที่นี้ได้นำเหล็กกล้าไร้สนิมเกรด SUS 304 และ SUS 447J1 ไปปล่อยไว้ในบรรยากาศเขตเมืองอุตสาหกรรมของเมืองชิบะ (Chiba) ประเทศญี่ปุ่น เป็นเวลา 7 และ 61 วันในช่วงฤดูกาลที่ต่างกัน จากนั้นนำมาทดลองทางไฟฟ้าเคมีเพื่อวัดศักย์ไฟฟ้าการเกิดรูเข็ม (pitting potential) และศักย์ไฟฟ้ากัดกร่อน (corrosion potential) วิเคราะห์ฟิล์มพาสซีฟด้วยเครื่องมือ Auger Electron Spectroscopy (AES) เพื่อตรวจวัดความหนาและวิเคราะห์ฟิล์มพาสซีฟด้วยเครื่องมือ X-ray Photoelectron Spectroscopy (XPS) เพื่อตรวจวัดการเปลี่ยนแปลงของส่วนผสมทางเคมี ผลการทดลองพบว่า เมื่อนำเหล็กกล้าไร้สนิมทั้งเกรด SUS 304 และ SUS 447J1 ไปปล่อยไว้ในบรรยากาศไฟฟ้าการเกิดรูเข็มและศักย์ไฟฟ้ากัดกร่อนสูงขึ้นจากกรณีที่ไม่ได้นำไปปล่อยไว้ในบรรยากาศ และกรณีปล่อยไว้ในบรรยากาศเป็นเวลาเท่ากัน ศักย์ไฟฟ้าการเกิดรูเข็มและศักย์ไฟฟ้ากัดกร่อนของเหล็กกล้าไร้สนิมเกรด SUS 447J1 สูงกว่าศักย์ไฟฟ้าการเกิดรูเข็มและศักย์ไฟฟ้ากัดกร่อนของเหล็กกล้าไร้สนิมเกรด SUS 304 สำหรับเหล็กกล้าไร้สนิมเกรด SUS 304 ที่นำไปปล่อยไว้ในบรรยากาศพบว่า สัดส่วนไอออนโครเมียมต่อไอออนเหล็กในฟิล์มพาสซีฟ (chromium enrichment) สูงขึ้น ขณะที่ความหนาของฟิล์มพาสซีฟลดลง นอกจากนี้สัดส่วนความเข้มข้นไฟโตอิเล็กตรอนของ H_2O และ OH ต่อ O^{2-} ของเหล็กกล้าไร้สนิมเกรด SUS 304 ที่ปล่อยไว้ในบรรยากาศเป็นเวลา 7 วัน ลดลงจากสัดส่วนที่ไม่ปล่อยทิ้งไว้ในบรรยากาศ แต่เมื่อนำไปปล่อยไว้ในบรรยากาศเป็นเวลา 61 วัน สัดส่วนดังกล่าวมีค่าใกล้เคียงกับกรณีที่ไม่ปล่อยทิ้งไว้ในบรรยากาศ จากผลการทดลองดังกล่าวสันนิษฐานว่า เกิดการพดพาฟิล์มพาสซีฟที่ประกอบด้วย H_2O และ OH ออกจากฟิล์มเมื่อนำเหล็กกล้าไร้สนิมเกรด SUS 304 ไปปล่อยไว้ในบรรยากาศเขตเมืองอุตสาหกรรมเป็นเวลา 7 และ 61 วัน และเกิดการสร้างไฮดรอกไซด์ในฟิล์มพาสซีฟของเหล็กกล้าไร้สนิมเกรด SUS 304 ที่ปล่อยไว้ในบรรยากาศเป็นเวลา 61 วัน หากพิจารณาว่าการปล่อยเหล็กกล้าไร้สนิมเกรด SUS 304 ในบรรยากาศเป็นเวลา 7 และ 61 วันเป็นไปอย่างต่อเนื่อง อาจสันนิษฐานได้ว่าเกิดการสร้างฟิล์ม H_2O และ OH ขึ้นมาระหว่างช่วงเวลาดังกล่าว และฟิล์มที่สร้างขึ้นมานั้น สามารถต้านทานการถูกพดพาออกมากขึ้นเมื่อเทียบกับฟิล์มพาสซีฟของชิ้นงานแรกที่ได้รับ (as-received) จากการศึกษาข้างต้นทำให้เสนอแนวความคิดว่า สัดส่วนไอออนโครเมียมที่สูงขึ้นและการเกิดขึ้นของไฮดรอกไซด์ในฟิล์มพาสซีฟของเหล็กกล้าไร้สนิมเกรด SUS 304 เมื่อนำไปปล่อยไว้ในบรรยากาศมีความสัมพันธ์กับศักย์ไฟฟ้าการเกิดรูเข็มและศักย์ไฟฟ้ากัดกร่อนที่สูงขึ้น กรณีของเหล็กกล้าไร้สนิมเกรด SUS 447J1 ที่นำไปปล่อยในบรรยากาศเป็นเวลา 7 และ 61 วัน เทียบกับกรณีที่ไม่ปล่อยทิ้งไว้ในบรรยากาศ ไม่ตรวจพบการเปลี่ยนแปลงที่เห็นได้ชัดของสัดส่วนไอออนโครเมียมต่อไอออนเหล็กในฟิล์มพาสซีฟและความหนาของฟิล์มพาสซีฟ แต่พบว่าสัดส่วนความเข้มข้นของไฟโตอิเล็กตรอนของ OH ต่อ H_2O , OH และ O^{2-} สูงขึ้น ผลการทดลองดังกล่าวทำให้เสนอแนวความคิดว่า การเกิดไฮดรอกไซด์ในฟิล์มพาสซีฟของเหล็กกล้าไร้สนิมเกรด SUS 447J1 เมื่อนำไปปล่อยไว้ในบรรยากาศมีความสัมพันธ์กับศักย์ไฟฟ้าการเกิดรูเข็มและศักย์ไฟฟ้ากัดกร่อนที่สูงขึ้น

ภาควิชา..... วิศวกรรมโลหการ.....ลายมือชื่อนิสิต.....สมฤกษ์ จันทรอัมพร.....
 สาขาวิชา..... วิศวกรรมโลหการ.....ลายมือชื่ออาจารย์ที่ปรึกษา.....ROY. WANN.....
 ปีการศึกษา.....2544.....

4270684021: MAJOR METALLURGICAL ENGINEERING

KEY WORD: PASSIVE FILM/SUS304/SUS447J1/PITTING POTENTIAL/
CORROSION POTENTIAL/AES/XPS

SOMRERK CHANDRA-AMBHORN: ANALYSIS OF PASSIVE FILMS
FORMED ON SUS304 AND SUS447J1 STAINLESS STEEL EXPOSED IN
AN URBAN-INDUSTRIAL ATMOSPHERE. ASSIST. PROF. GOBBOON
LOTHONGKUM, Dr.-Ing. ,43 pp. ISBN 974-03-0318-8.

The 2B-finished SUS 304 and SUS 447J1 stainless steels were atmospherically exposed to different seasons for 7 and 61 days in the Chiba urban-industrial site. The pitting and corrosion potentials of the samples were determined by an electrochemical technique. AES sputtering was applied to evaluate passive film thickness, and chemical compositions in passive film were investigated by XPS analysis. The pitting and corrosion potentials of SUS 304 and SUS 447J1 stainless steels increase after exposure. With the same exposure period, the pitting and corrosion potentials of SUS 304 stainless steels are lower than those of SUS 447J1 stainless steels. The passive film thickness of SUS 304 stainless steels after exposure decrease. The passive film of specimens exposed for 7 days is thinner than that of specimens exposed for 61 days. Cr enrichment in passive film increases after exposure, but the specimen exposed for 7 days has less Cr enrichment than that exposed for 61 days. By comparing with the unexposed specimen, after the 7-day exposure period the photoelectron intensity ratio of H_2O and OH^- per O^{2-} in passive film decreases, but it is nearly the same ratio after the 61-day exposure period. It is purposed that H_2O and OH^- film of SUS 304 stainless steel is removed after exposure for 7 and 61 days, and hydroxide was formed in passive film after the 61-day exposure period. By assuming that the 7-days exposure period represents an early stage of passive film change, the former H_2O and OH^- film of SUS 304 stainless steel may be removed after the 7-days exposure, and the new H_2O and OH^- film is continuously developed during the exposure for 7 and 61 days. This novel film has resistance to be removed by the environment that is superior to the H_2O and OH^- film of the unexposed specimen. For SUS 304 stainless steels, the Cr enrichment and the formation of hydroxide in passive film after exposure may relate to the positive shift of pitting and corrosion potentials. For SUS 447J1 stainless steels, the changes of Cr enrichment and passive film thickness cannot be considerably observed after the exposure periods of 7 and 61 days. However, the increase in the photoelectron intensities of OH^- per H_2O , OH^- and O^{2-} can be observed. The hydroxide film formed after exposures may relate to the positive shift of pitting and corrosion potentials.

Department.....Metallurgical Engineering...Student's signature.
Field of Study..Metallurgical Engineering...Advisor's signature
Academic Year.....2001.....

Somrerk Chandra-ambhorn
Gobboon Lothongkum

Acknowledgement

The financial support by Kawasaki Steel Corporation, Japan and National Science and Technology Development Agency, Thailand, is gratefully acknowledged. The author is gratefully indebted to Asst. Prof. Dr.-Ing. Gobboon Lothongkum for his kindly help and cooperation with Kawasaki Steel Corporation for the research sandwich program at the Technical Research Laboratory in Chiba City from November 2000 to April 2001. His acknowledgement is also extended to the chairman of committee Assoc. Prof. Dr. Prasonk Sricharoenchai and the member of committee Dr. Sawai Danchaivijit. The appreciated thanks also go to Dr. S. Satoh, Mr. A. Yamamoto and Mr. U. Usui for their helpful advice. The author had spent the wonderful times for a half year to work at the Chiba City under the supervision of Ms. N. Makiishi and Ms. M. Tochiara. The author wishes to give the special thank to them.

Finally, the author wishes to thank the AES operator, Mr. K. Suzuki, as the best friend during his staying in Japan. And last, but not least, no words can be sent to the author's mum and sisters for their warmly love and taking good care of him that he is always touched.



Table of Contents

	Page
Abstract (Thai).....	iv
Abstract (English).....	v
Acknowledgement.....	vi
Table of Contents.....	vii
List of Figures.....	ix
List of Tables.....	xi
Chapter	
I Introduction.....	1
1.1 Generalization	
1.2 Objectives	
1.3 Scopes of the work	
1.4 Advantages of the work	
II Literature Review.....	3
2.1 Introduction to SUS 304 and SUS 447J1 stainless steels	
2.2 Electrochemical behavior of passive film before and after atmospheric exposure	
2.3 Characterization of passive film	
2.3.1 Characterization of passive film before atmospheric exposure	
2.3.2 Characterization of passive film after atmospheric exposure	
2.4 Gel-like structure model and selected application	
III Experimental method.....	14
3.1 History and installation for exposure test of specimens	
3.2 Preparation of specimens	
3.3 Experimental procedures	
3.3.1 Measurement for pitting and corrosion potential	
3.3.2 AES analysis	
3.3.3 XPS analysis	
IV Results and Discussion.....	17
4.1 Effects of stainless steel compositions and exposure periods on the pitting and corrosion potentials	
4.2 Effects of stainless steel compositions and exposure periods on the thickness of passive film	
4.3 Effects of stainless steel compositions and exposure periods on the composition of passive film	
4.3.1 The Fe and Cr compositions	
4.3.2 The Ni and Mo compositions	
4.3.3 The oxygen distribution	
4.4 Schematic sketch of the change in construction of passive film of SUS 304 and SUS 447J1 stainless steels before and after atmospheric exposure for 7 days and 61 days	
4.5 Photo-inhibition under UV and natural light irradiation	

List of Contents (continued)

	Page
V Conclusions.....	34
References.....	35
Appendices	
Appendix 1 Principle of X-ray Photoelectron Spectroscopy.....	38
and Auger Electron Spectroscopy	
A1.1 X-ray Photoelectron Spectroscopy	
A1.2 Auger Electron Spectroscopy	
Appendix 2 XPS Quantification by using Relative Sensitivity Factor.....	40
Appendix 3 Experiment for investigating the accuracy of	
XPS Quantification by using Relative Sensitivity Factor.....	41
A3.1 Objectives	
A3.2 Scope	
A3.3 Experimental Method	
A3.3.1 Specimens	
A3.3.2 XPS analysis	
A3.4 Results	
A3.5 Conclusions	
Vitae.....	43

จุฬาลงกรณ์มหาวิทยาลัย

List of Figures

	Page
Figure 2.1: Corrosion resistance of stainless steels including SUS304 and SUS447J1 stainless steel.....	4
(a) % Rust area as a function of pitting index	
(b) Pitting potential, V'_{c10} , as a function of pitting index	
Figure 2.2: Pitting potential as a function of (a) %Cr and (b) %Mo in bulk composition	5
Figure 2.3: Corrosion potential of 2B-finished AISI304 stainless steel as a function of exposure period in Milan urban-industrial site	6
Figure 2.4: Pitting potential of 2B-finished AISI304, AISI430 and AISI316 stainless steel as a function of exposure period in Milan urban-industrial site.....	6
Figure 2.5: Mass concentration of Cr in passive film and substrate immediately under passive film as a function of Cr content in bulk composition.....	7
Figure 2.6: Passive film thickness of mechanically polished Fe and Fe-Cr alloy and Cr as a function of Cr in bulk composition.....	8
Figure 2.7: intensities of emitted photoelectron as a function of sputtering time of SUS304 stainless steel.....	8
Figure 2.8: The schematic sketch of passive film model of SUS304 stainless steel....	9
Figure 2.9: XPS spectra of Ni2p _{3/2} , Fe2p _{3/2} and Cr2p _{3/2} of 20Cr-18Ni-6Mo-0.2N at the take-off angle of 10°, 38.5° and 80°	9
Figure 2.10: The schematic sketch of passive film stainless steels containing 20-29%Cr and 4-29%Ni exposed in air lasted for 24 hours.....	10
Figure 2.11: The average of cationic fraction of Cr in passive film of SUS304 and SUS316 austenitic stainless steels at Miyakojima subtropical site and Kinu-ura temperate site for 6 months.....	11
Figure 2.12: The average of cationic fraction of Cr in passive film of SUS430 and SUS444 ferritic stainless steels at Miyakojima subtropical site and Kinu-ura temperate site for 6 months	11
Figure 2.13: AES depth profile of 2B-finished SUS304 exposed in Shinomisaki marine site lasted for 5 years.....	12
Figure 2.14: Schematic sketch of the process of the formation of passive film according to gel-like structure model.....	13
Figure 3.1: AES micrograph of as-received 2B-finished SUS304 stainless steel.....	14
Figure 3.2: AES micrograph of as-received 2B-finished SUS447J1 stainless steel.....	14
Figure 4.1: Pitting potential of SUS304 stainless steels exposed for 7 days and 61 days in Chiba urban-industrial site.....	17
Figure 4.2: Pitting potential of SUS447J1 stainless steels exposed for 7 days and 61 days in Chiba urban-industrial site.....	18
Figure 4.3: Corrosion potential of SUS304 and SUS447J1 stainless steels unexposed and exposed for 7 days in Chiba urban-industrial site.....	19
Figure 4.4: AES depth profile of Fe, O, Cr and Ni Auger electron intensity as a function of sputtering time of as-received SUS304 stainless steel....	19

List of Figures (continued)

	Page
Figure 4.5: AES depth profile of O_{KLL} Auger electron intensity of as-received SUS304 and SUS447J1 stainless steels as a function of sputtering time.....	20
Figure 4.6: AES depth profile of O_{KLL} Auger electron intensity of SUS304 stainless steel before and after exposed for 7 days and 61 days in Chiba urban-industrial site.....	21
Figure 4.7: AES depth profile of O_{KLL} Auger electron intensity of SUS447J1 stainless steel before and after exposed for 7 days and 61 days in Chiba urban-industrial site.....	21
Figure 4.8: XPS spectrum of $Fe2p_{3/2}$ of as-received SUS304 stainless steel.....	22
Figure 4.9: XPS spectrum of $Cr2p_{3/2}$ of as-received SUS304 stainless steel.....	23
Figure 4.10: XPS spectra of $Fe2p_{3/2}$, $Cr2p_{3/2}$, $Ni2p_{3/2}$ and $O1s$ of SUS304 stainless steel at different exposure periods.....	24
Figure 4.11: XPS spectra of $Fe2p_{3/2}$, $Cr2p_{3/2}$, $Mo2d_{3/2,5/2}$ and $O1s$ of SUS447J1 stainless steel at different exposure periods.....	25
Figure 4.12: Cr enrichments in passive films of SUS304 and SUS447J1 stainless steels at different exposure periods.....	26
Figure 4.13: XPS spectrum of $Ni2p_{3/2}$ of as-received SUS304 stainless steel.....	26
Figure 4.14: Ni enrichments in passive films of SUS304 stainless steel at different exposure periods.....	27
Figure 4.15: XPS spectrum of $Mo2d_{3/2,5/2}$ of as-received SUS447J1 stainless steel...27	27
Figure 4.16: $O1s$ spectrum of as-received SUS304 stainless steel.....	28
Figure 4.17: The photoelectron intensities of OH^- and H_2O per O^{2-} of SUS304 stainless steel at the different exposure periods.....	28
Figure 4.18: The photoelectron intensities of OH^- per H_2O , OH^- and O^{2-} of SUS447J1 stainless steel at the different exposure periods.....	29
Figure 4.19: Schematic sketch of the change in construction of passive film of SUS304 and SUS447J1 stainless steels.....	31
Figure A1.1: Schematic diagram of photoelectric effect excited by primary X-ray...38	38
Figure A1.2: Schematic diagram of Auger process excited by primary electron.....	39

List of Tables

	Page
Table 2.1: Chemical compositions of SUS304 and SUS447J1 stainless steels.....	3
Table 2.2: Mechanical and physical properties of SUS304 and SUS447J1 stainless steels.....	4
Table 2.3: Passive film thicknesses of austenitic and ferritic stainless steels before and after atmospheric exposure at Miyakojima subtropical site and Kinu-ura temperate site for 6 months.....	10
Table 3.1: Mass percent composition of as-received SUS304 and SUS447J1 stainless steels.....	15
Table A3.1: Mass percent of standard stainless steels used.....	41
Table A3.2: Raw area obtained from standard stainless steels.....	42
Table A3.3:RSFs and % accuracy of a measurement.....	42



สถาบันวิทยบริการ
 าลงกรณ์มหาวิทยาลัย

CHAPTER I

INTRODUCTION

1.1 Generalization

In addition to the mechanical properties, the corrosion resistances to an aggressive or a polluted atmosphere as well as the aesthetic surface play the important role for the selection and design of the architectural construction materials. Stainless steel due to its corrosion resistance and appreciated surface has been considered as one of the alternative materials for serving those purposes. SUS 304 austenitic stainless steel mainly alloyed with 18-wt% Cr and 8-wt% Ni is a conventional grade for a weathering purpose. However, some grades have been developed to attain the superior properties especially the corrosion resistance. The SUS 447J1 ferritic stainless steel (1-4) mainly alloyed with 30-wt% Cr and 2-wt% Mo is an interesting one. The example of its application is the roof of the Kansai International Airport in Japan. (2)

It is well accepted that the passive film formed on stainless steels plays the vital role for the corrosion resistance. (5-8) Many works reported the existence of oxy-hydroxide in passive film. (5,6,9-11) The change of passive film of the as-received stainless steels with different surface finishes (8), immersed in various solutions (12), implanted by molybdenum (10), and atmospherically exposed (7,8,13) were investigated. However, the different results were reported for the atmospheric exposure, for instances, the decrease (8) and increase (13) in Cr enrichment in passive film as well as the decrease (13) and increase (8) in passive film thickness after atmospheric exposure. Those results should not be over emphasized because of the different stainless steels studied, different experimental conditions and analysis methods used. The interesting questions are still remained for the atmospheric exposed stainless steels. What are their pitting and corrosion potentials, chemical compositions and thickness of passive film? How is their corrosion resistance changed and by what mechanisms? The investigation of SUS 304 stainless steel surface subjected to the atmospheric exposure was extensively carried out by both electrochemical and surface analysis. (5,7,8,10,13) However, a few attentions were paid to those of SUS 447J1 stainless steel. In the present work, the common used 2B-finished SUS 304 and SUS 447J1 stainless steels were atmospherically exposed in Chiba urban-industrial site for 7 days and 61 days. The electrochemical measurements accompanied by surface analysis methods, AES and XPS, were then applied to investigate the pitting and corrosion potential, film thickness and chemical composition in passive film of specimens before and after those exposures. The phenomena were firstly clarified, and mechanisms were then discussed.

1.2 Objectives

1. To investigate the changes of pitting and corrosion potentials of SUS 304 and SUS 447J1 stainless steels before and after atmospheric exposure.
2. To investigate the change of passive film thickness of SUS 304 and SUS 447J1 stainless steels before and after atmospheric exposure by using Auger electron spectroscopy.

3. To investigate the change of chemical compositions of alloying elements and oxygen in passive film of SUS 304 and SUS 447J1 stainless steels before and after atmospheric exposure by using X-ray photoelectron spectroscopy.

4. To explore the possible mechanisms of the change of passive film related to the corrosion resistance represented by pitting and corrosion potentials of SUS 304 and SUS 447J1 stainless steels after exposure in atmosphere.

1.3 Scopes of the work

1. The exposure periods were 7 days in January 2001, and 61 days during August 22nd to October 22nd, 2000.

2. The selected exposure site was the Chiba urban-industrial site situated 1 km far from the seafront.

3. Anodic polarization was applied to determine the pitting potentials. The 3.5-g/cm³ NaCl solution was maintained at 30°C as for SUS 304 stainless steel and at 70°C for SUS 447J1 stainless steel.

4. AES depth profile of oxygen and iron distribution as a function of sputtering time was used to estimate passive film thickness with the sputtering rate same as that for pure iron.

5. XPS quantification was carried out by using relative sensitivity factor obtained from standard stainless steels.

1.4 Advantages of the work

1. Be able to understand the change of chemical compositions of passive film and passive film thickness related to the change of pitting and corrosion potentials of SUS 304 and SUS 447J1 stainless steels after exposure in the atmosphere of Chiba urban-industrial site for 7 days and 61 days.

2. The possible mechanisms of the change of passive film of SUS 304 and SUS 447J1 stainless steels after exposure in the atmosphere of Chiba urban-industrial site for 7 days and 61 days were discussed. The understanding of the corrosion behavior of SUS 304 and SUS 447J1 stainless steels with respect to the in-depth change of passive film are expected.

CHAPTER II

LITERATURE REVIEW

First of all, SUS 304 and SUS 447J1 stainless steels are introduced. Then, the electrochemical properties of both grades before and after atmospheric exposure are re-examined. Subsequently, it is the reviews of film thickness and chemical compositions of passive film of stainless steels both before and after atmospheric exposure. One of possible mechanism of passive film formation, gel-like structure model, is also finally discussed.

2.1 Introduction to SUS 304 and SUS 447J1 stainless steels

The conventional SUS 304 and SUS 316 austenitic stainless steels are often used for architectural purpose. This is mainly because their corrosion resistance is better than the conventional ferritic stainless steel, such as SUS 430 ferritic stainless steel. (2) SUS 304 stainless steel consists mainly of 18-wt% Cr and 8-wt% Ni same as SUS 316 but Mo ca. 2 wt% is added in SUS 316 austenitic stainless steel for increasing the pitting corrosion resistance. (14) To improve the corrosion resistance of ferritic stainless steel as well as the other properties, some elements are alloyed for developing the novel grades. SUS 447J1 ferritic stainless steel was developed by the principal alloying of 30-wt% Cr and 2-wt% Mo to promote the corrosion resistance. (2,3) Furthermore, around 0.1 wt% Ni is added for the convenient production, especially to promote the enough toughness for rolling. (15) Chemical compositions of SUS 304 and SUS 447J1 are shown in Table 2.1. The corrosion, mechanical and physical properties of both grades will be further discussed in detail.

Table 2.1 Chemical compositions of SUS 304 and SUS 447J1 stainless steels (2)

Steel	Mass%								
	C	Si	Mn	P	S	Cr	Ni	Mo	N
SUS304	0.06	0.32	1.02	0.031	0.005	18.2	8.5	0.2	0.02
SUS447J1	0.003	0.13	0.11	0.02	0.004	29.6	0.1	2.09	0.006

For testing the general corrosion resistance of SUS 304 and SUS 447J1 stainless steels, the 2B-finished surface was exposed for 1.5 years to the atmosphere in Chiba coastal industrial site. The samples were placed 4 meters away from the seafont. The rust area of the tested samples were evaluated and plotted against the pitting index ($\%Cr + 3x\%Mo$), which is around 18 and 36 for SUS 304 and SUS 447J1 stainless steels, respectively. The results showed in Figure 2.1(a). This Figure illustrates that, after exposure in the mentioned condition, all exposure area of SUS 304 stainless steel completely rusts, whereas all area of SUS 447J1 stainless steel surface (R30-2) is absolutely immune.

Pitting potentials, as the corrosion resistance indicator, of the tested steels in 3.5-wt% NaCl aqueous solution at 70°C using standard calomel electrode as the reference electrode was also investigated by potentiodynamic method. Potentials that current density reaches $10 \mu A/cm^2$, $V \times 10$, were recorded as pitting potentials and plotted related to pitting index as shown in the Figure 2.1(b). It can be seen that pitting potentials of SUS 304 stainless steel are less than $200 mV_{SCE}$, whereas those

of SUS 447J1 stainless steel are around 600 mV_{SCE}. It is apparent from Figure 2.1 that corrosion resistance, represented by percentage of rust area and pitting potentials, of SUS 447J1 stainless steel is higher than that of SUS 304 stainless steel.

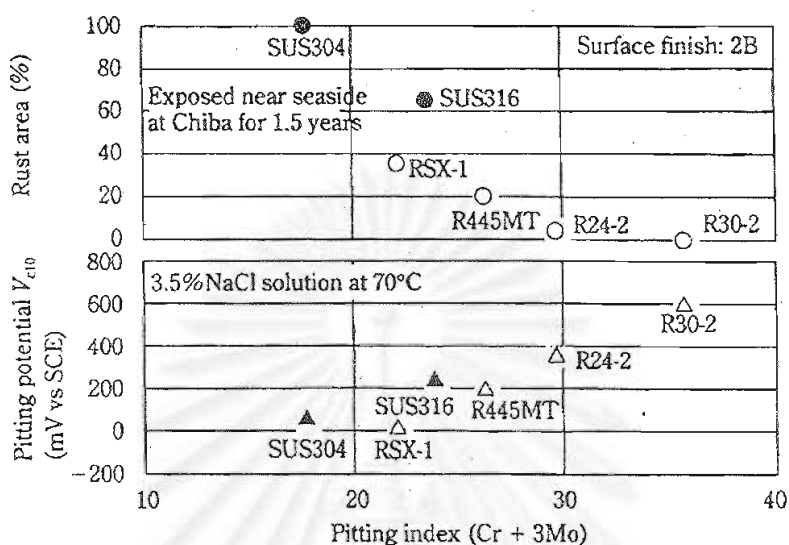


Figure 2.1 Corrosion resistance of SUS 304 and SUS 447J1 stainless steels (2)

(a) % Rust area vs. pitting index

(b) Pitting potentials, V'c10, vs pitting index

Table 2.2 summarized the mechanical and physical properties of SUS 304 and SUS 447J1 stainless steels. It was reviewed that (2) SUS 447J1 stainless steel can be applied such as panel or roofing member by ordinary bending, press forming or rolled forming. Due to smaller thermal expansion and greater thermal conductivity of SUS 447J1 stainless steel than those of SUS 304 stainless steel, the thermal stress in SUS 447J1 stainless steel caused by welding or temperature change day and night decrease. The improved properties of SUS 447J1 stainless steel are attractive for serving as a long panel or roofing. The example application of SUS 447J1 stainless steel is the roof of Kansai International Airport, the first offshore airport in Japan.

Table 2.2 Mechanical and physical properties of SUS 304 and SUS 447J1 stainless steels (2)

Steel	Yield strength (MPa)	Tensile strength (MPa)	% Elongation	Thermal conductivity (W/mK)	Coefficient of thermal expansion between 273 to 573 K ($10^{-6}/K$)	Density (g/cm^3)
SUS304	284	637	58	16.2	16	7.93
SUS447J1	430	539	30	18.9	9.6	7.64

2.2 Electrochemical behavior of passive film before and after atmospheric exposure

Yoshihiro Kasawa, and et.al., (3) investigated the effects of Cr and Mo on pitting potentials of stainless steels contained 11-30 wt% Cr and 0-4 wt% Mo in 3.5-wt% NaCl aqueous solution at 30°C by potentiodynamic method and using standard calomel electrode as the reference electrode. The potentials at a current density of $10 \mu\text{A}/\text{cm}^2$, V'_{c10} , was selected as pitting potentials. The relationship between V'_{c10} as a function of %Cr and %Mo is illustrated in Figure 2.2.

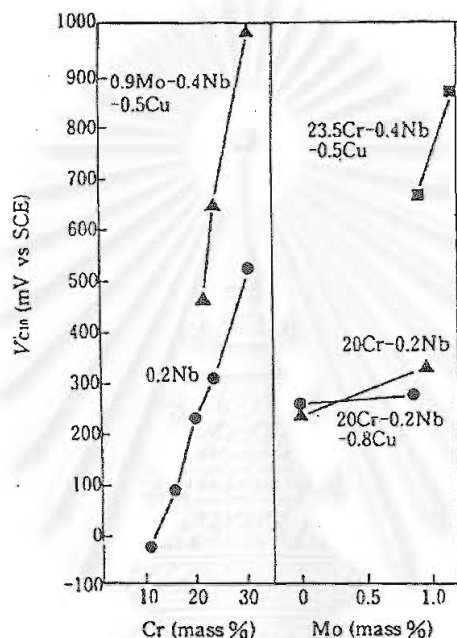


Figure 2.2 Pitting potentials as a function of (a) %Cr (b) %Mo of stainless steels (3)

It can be seen that pitting potentials of 0.9Mo-0.4Nb-0.5Cu stainless steel and 0.2 Nb stainless steel distinguishably increases as Cr contents in bulk composition increases. Pitting potential also increases with the increase in %Mo in bulk composition in the case of 23.5Cr-0.4Nb-0.5Cu, 20Cr-0.2Nb and 20Cr-0.2Nb-0.8Cu stainless steels. By considering that the increase in pitting potential indicate the capability for suppressing the generation of pit, the authors (3) purposed the role of Cr and Mo on the suppression of pit generation. However, how Cr and Mo physically take part in passive film was not clearly explored in this work.

N. Azzari (7) studied the corrosion and pitting potentials of 2B-finished SUS 304 (AISI 304) stainless steel subjected to atmosphere in Milan urban-industrial site for 3 years. Some specimens were then picked up at any period and without any surface treatment immersed in 0.5-M NaCl solution at 45°C to evaluate the corrosion and pitting potentials. The results from electrochemical measurement are shown in Figure 2.3. It is apparent that corrosion potentials increase with increasing time in the first two years. The curve is a parabolic form. Azzari suggested that the relation is $E_{\text{corr.}} = 220 - 360t^{0.43}$. Pitting potentials of the same specimens were also investigated. Figure 2.4 illustrates pitting potentials of AISI 304, AISI 430 and AISI 316 stainless steels as a function of atmospheric exposure time. It appears that pitting potentials, therefore the corrosion resistance increases with the increase in

atmospheric exposure time until 24 months afterwards the deterioration of pitting potentials of all stainless steels grade can be observed. Its validity for service seems to be unaccepted after the exposure period exceeds around 24 months. The author purposed the role of water adsorption and the absorption of anions on the degradation of passive film. This will be discussed later in section 2.4.

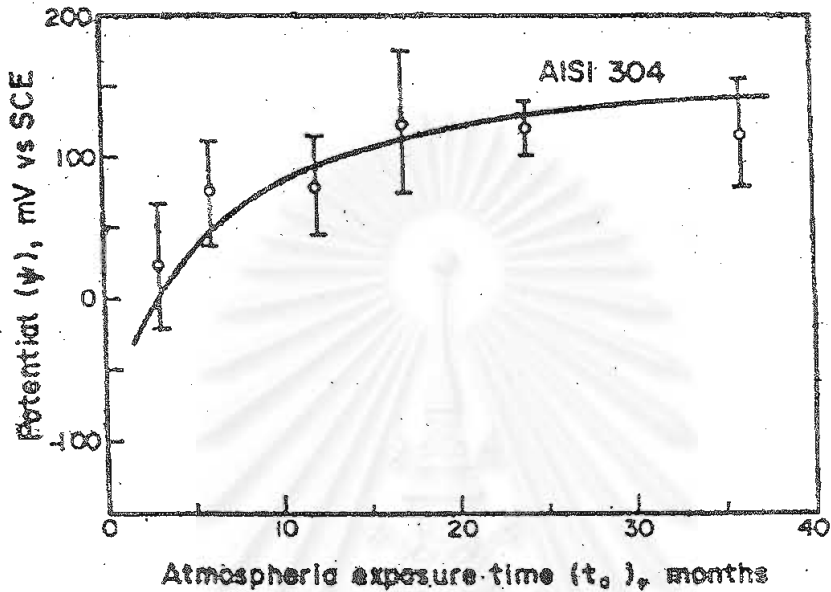


Figure 2.3 Corrosion potentials of 2B-finished AISI 304 stainless steel as a function of the exposure time in Milan urban-industrial site (7)

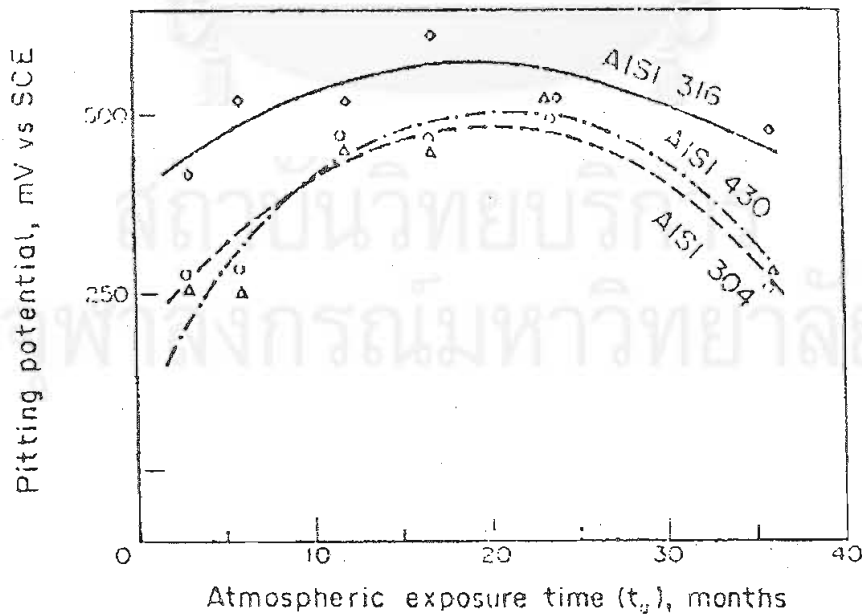


Figure 2.4 Pitting potentials of 2B-finished AISI 304, AISI 430 and AISI 316 stainless steels as a function of exposure time in Milan urban-industrial site (7)

2.3 Characterization of passive film

2.3.1 Characterization of passive film before atmospheric exposure

K. Asami et. al. (16) studied the composition and structure of passive film formed on a series of Fe-Cr alloy in de-aerated 1-M H_2SO_4 solution by using XPS quantitatively. The change of composition of passive film and alloy adjacent to passive film on Fe-Cr alloy polarized at 100 and 500 mV_{SCE} as a function of alloy composition are illustrated in Figure 2.5. The circle mark represents the cationic fraction of Cr in passive film, whereas the triangle mark represents the cationic fraction of Cr in the alloy surface of substrate just under passive film. The solid mark represents coordinate corresponding to specimen polarized at 100 mV_{SCE}, whereas the hollow mark indicates the polarization at 500 mV_{SCE}. This Figure reveals that Cr content of passive film increases drastically at ca. 13-wt.% Cr of the bulk composition. However, no Cr enrichment had been found in the surface of substrate next to passive film.

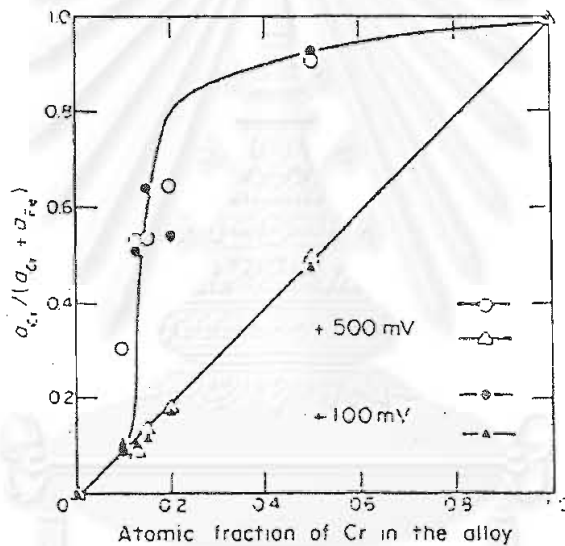


Figure 2.5 Mass concentration of Cr in passive film and substrate immediately under passive film as a function of Cr content in bulk composition (16)

K. Asami, and et.al, (17) also investigated the effect of atomic fraction of Cr in Fe-Cr alloy on the thickness of passive film by using XPS. The specimen was polished with SiC abrasive paper in Trichloroethylene, and then clean ultrasonically before XPS measurement. Figure 2.6 illustrates the thickness of passive film of Fe-Cr alloy as a function of Cr in bulk composition. Film thickness increases to the maximum when the Cr atomic fraction of bulk composition reaches ca. 13 atomic percent.

E. De Vito and P. Marcus (10) purposed the elemental distribution models of passive film for SUS 304 stainless steel using XPS sputtering technique. Figure 2.7 illustrates intensities of the emitted photoelectrons as a function of sputtering time of SUS 304 stainless steel. The total sum of Fe^{2+} and Fe^{3+} was taken from depth profile because of two reasons. The full width at half maximum (FWHM) of iron oxide spectrum is large comparing to the difference of the binding energy between Fe^{3+} and Fe^{2+} , and the reduction of Fe^{3+} and Fe^{2+} by ion sputtering cannot be ignored.

From Figure 2.7, it can be seen that chromium hydroxide appears to be located in the outer part of passive film. The increasing signal of oxide states of Fe and Cr indicates their location in the inner part of passive film. The enrichment of chromium oxide near the film/alloy interface can be observed.

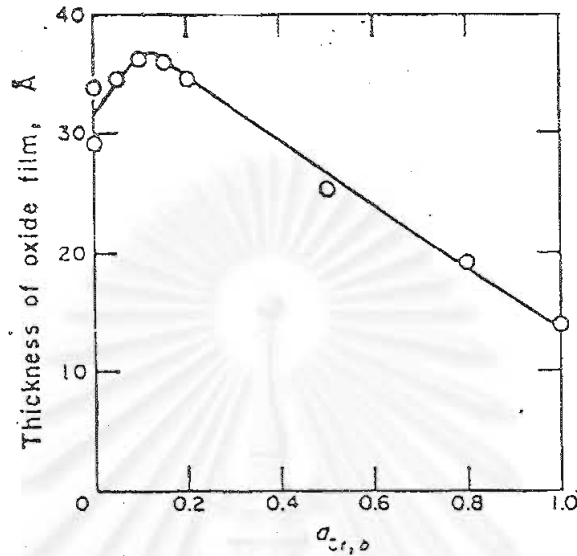


Figure 2.6 Passive film thickness of mechanically polished Fe and Fe-Cr alloy and Cr as a function of Cr in bulk composition (17)

The authors (10) also proposed the passive film model of SUS 304 stainless steel as depicted in Figure 2.8. This schematic sketch illustrates the covering of contamination with the thickness of 0.6 nm on the top surface. Passive film is divided into 3 layers. The layer of chromium hydroxide forms on the layer of iron oxide and chromium oxide, which iron oxide co-exists with chromium oxide by the ratio of 31:69. The layer of iron oxide and chromium oxide forms on the layer of Cr^0 and Ni^0 , which Cr^0 co-exists with Ni^0 by the ratio of 60:40. The estimated thicknesses of compound layers are 0.6 nm, 0.8 nm and 0.3 nm respectively.

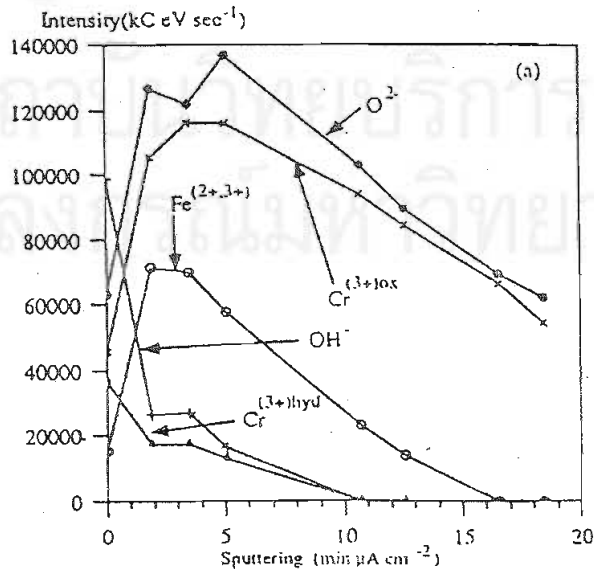


Figure 2.7 Intensities of emitted photoelectron as a function of sputtering time of SUS 304 stainless steel (10)

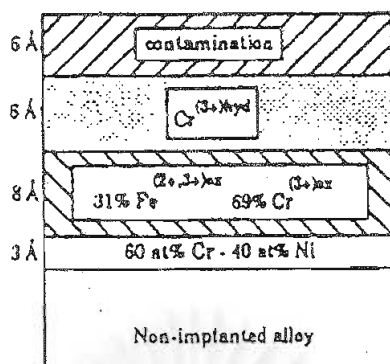


Figure 2.8 Schematic sketch of passive film model of SUS 304 stainless steel (10)

I. Olefjord and L. Wegelius (9) applied XPS technique to investigate chemical compositions of passive film of 20Cr-18Ni-6Mo-0.2N polarized in 0.1-M HCl + 0.4-M NaCl solution. The specimens were cathodically treated at -600 mV_{SCE} for 30 minutes and then polarized at 500 mV_{SCE} for 10 minutes. XPS spectra of Ni2p_{3/2}, Fe2p_{3/2} and Cr2p_{3/2} at the take-off angle of 10°, 38.5° and 80° are illustrated in Figure 2.9. It can be seen that Ni⁰ is dominating, whereas Ni²⁺ is low. The chromium oxidation state is trivalent. They are Cr³⁺ bounded to OH⁻ denoted as Cr³⁺(hyd), Cr²⁺ bounded to O²⁻ denoted as Cr²⁺(ox), and Cr⁰ is metallic state. It appears that the photoelectron ratio of Cr³⁺(hyd) per Cr²⁺(ox) is largest at the lowest take-off angle. This indicates that the location of Cr³⁺(hyd) is in the outer part and that of Cr²⁺(ox) is in the inner part of passive film. O1s spectra are deconvoluted to be 3 peaks representing oxygen in O²⁻, OH and H₂O. The ratio of OH⁻/O²⁻ photoelectron decreases with the increase in take-off angle indicating the location of hydroxide in the outer side compared to oxide in passive film.

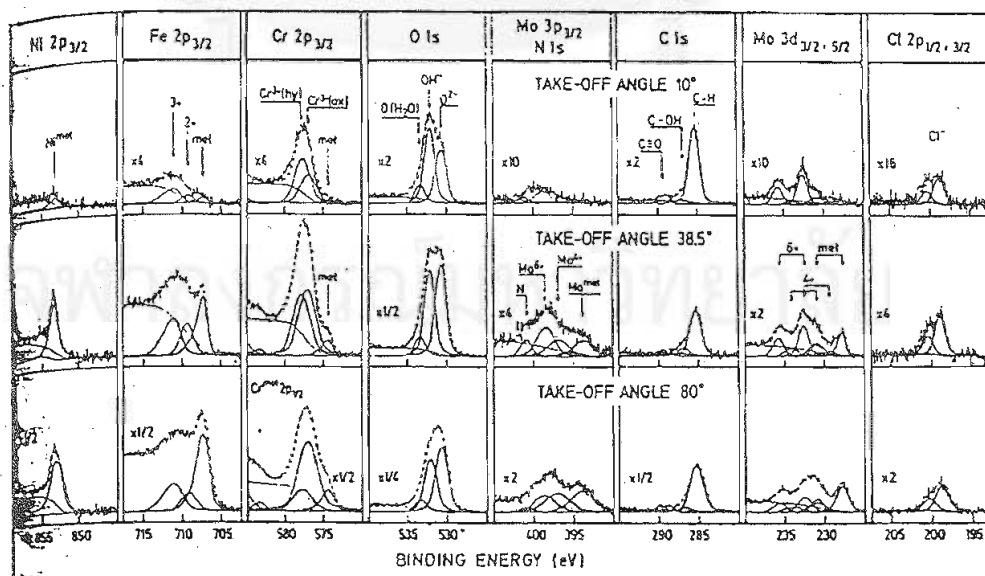


Figure 2.9 XPS spectra of Ni2p_{3/2}, Fe2p_{3/2} and Cr2p_{3/2} of 20Cr-18Ni-6Mo-0.2N at the take-off angle of 10°, 38.5° and 80° (9)

S. Chaikittisilp (11) applied XPS technique to analyze the passive films of ferritic and austenitic stainless steels containing 20-29%Cr and 4-29%Ni exposed in air for 24 hours. The schematic sketch of passive film of these specimens is depicted in Figure 2.10. Passive film can be distinguished to be 2 layers that are chromium hydroxide and chromium oxide layers. The estimated thickness of chromium hydroxide layer is around 0.15 nm. The chromium oxide layers can be further divided into 2 layers. The top layer consists of chromium oxide, iron oxide and iron with the estimated thickness of 0.5 to 2.5 nm. The lower layer contains chromium oxide, chromium, iron and nickel with the estimated thickness of 0.9 to 3.5 nm. It was also found that the increase in Cr content in bulk composition results in the decrease in passive film thickness but the increase in the layer that contains chromium oxide, iron oxide and iron.

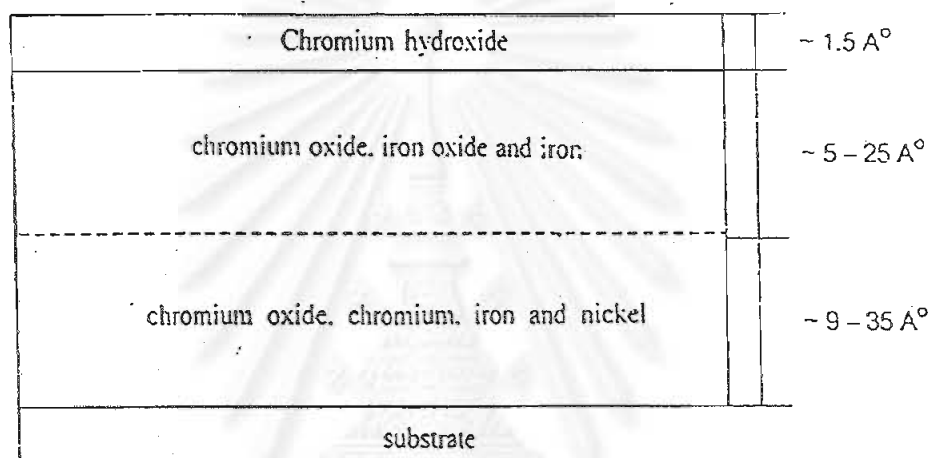


Figure 2.10 Schematic sketch of passive film stainless steels containing 20-29%Cr and 4-29%Ni exposed in air for 24 hours (11)

2.3.2 Characterization of passive film after atmospheric exposure

In K. Asami and H. Hashimoto's work (8), 2B-finished SUS 304 and SUS 430 stainless steels and MR-finished SUS 316 and SUS 444 stainless steels were exposed at the Miyakojima subtropical site and the Kinu-ura site for 6 months. The passive film thickness and chemical compositions in passive film were quantitatively investigated by XPS. The passive film thicknesses of austenitic and ferritic stainless steels are reported in Table 2.3.

Table 2.3 Passive film thickness of austenitic and ferritic stainless steels before and after atmospheric exposure at the Miyakojima subtropical site and the Kinu-ura site for 6 months (8)

Exposure site	Passive film thickness (nm)			
	Average of austenitic stainless steels		Average of ferritic stainless steels	
	Thickness	Increment	Thickness	Increment
Unexposure	2.48	-	2.91	-
Miyakojima	4.08	1.60	4.68	1.77
Kinu-ura	3.94	1.45	4.59	1.68

It can be seen that passive film thickness of both types increase after exposure. Passive film thickness of ferritic stainless steel is higher than that of austenitic stainless steel before and after atmospheric exposure in both sites. The increments are larger at the Miyakojima site than at the Kinu-ura site. The authors suggested the effects of temperature and NaCl deposition rate on surface on the difference in the change of film thickness of specimens exposed in different sites. In the case of the Miyakojima subtropical site, average annual temperature is around 296 K and NaCl deposition rate is 1.1 to 1.6 (mg/dm²)/day. In the case of the Kinu-ura temperate site, the environment parameter is similar to that of the Choshi site, which the average temperature is lower than ca. 283 K and NaCl deposition rate is around a half of that of Miyakojima site. The average of cationic fraction of alloying elements in passive film of SUS 304 and SUS 316 austenitic stainless steels is illustrated in Figure 2.11, and the average of cationic fraction of Cr in passive film of SUS 430 and SUS 444 ferritic stainless steels is illustrated in Figure 2.12. These two Figures indicate the diminishing of Cr in passive film after exposure.

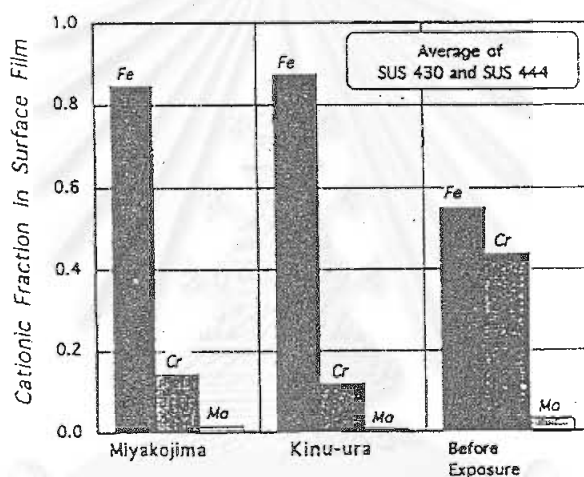


Figure 2.11 The average of cationic fraction of Cr in passive film of SUS 304 and SUS 316 austenitic stainless steels at the Miyakojima subtropical site and the Kinu-ura temperate site for 6 months (8)

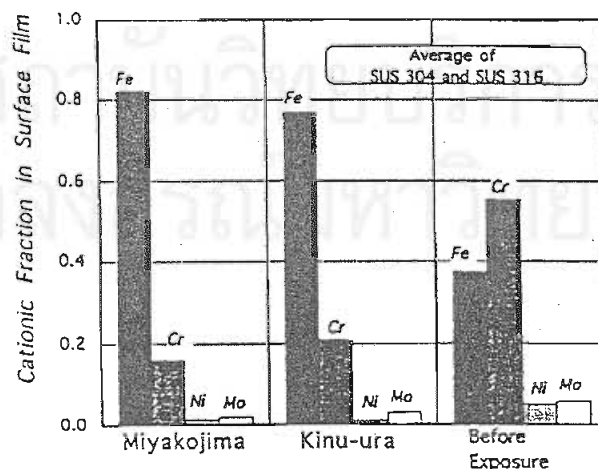


Figure 2.12 The average of cationic fraction of Cr in passive film of SUS430 and SUS 444 ferritic stainless steels at Miyakojima subtropical site and Kinu-ura site for 6 months (8)

However, M. Tochiara (13) confirmed the increase in Cr enrichment of 2B-finished SUS 304 stainless steel after the long-term exposure. Cr content in passive film of 2B-finished SUS 304 stainless steel exposed to the Shinomisaki marine site for 5 years was investigated by AES sputtering technique as illustrated in Figure 2.13. The auger electron-intensity ratios of Cr/Fe were plotted vs. sputtering time. It can be seen that, after exposure, Cr enrichment in passive film increases but film thickness decreases.

An interesting question should be noted. What is the relationship between the changes of pitting and corrosion resistance, passive film thickness, and the existence of elements or compounds in passive film and after stainless steels were exposed to any atmosphere? In the case of unexposed stainless steels, the effect of Cr in passive film plays the important role for the increase in pitting potentials as described in section 2.2. The previous survey also points that after the certain exposure period pitting potentials increase but how the change of Cr enrichment in passive film is unclear. It should not be over emphasized about those results because they were obtained from the different experiments. In the present work, the pitting and corrosion potentials obtained from electrochemical measurement and surface analysis results from AES and XPS will be integrated in one set of experiment to discuss the relationship.

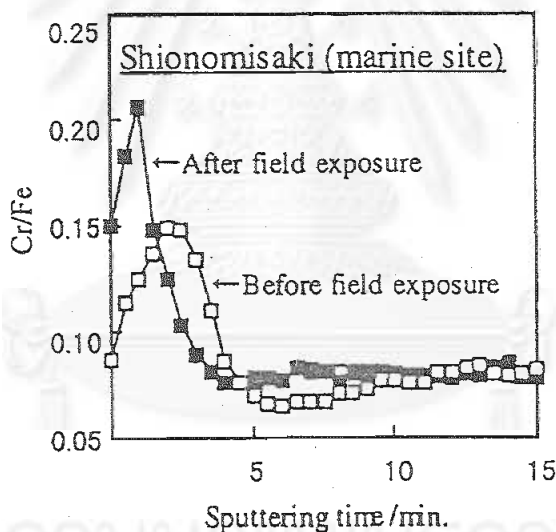


Figure 2.13 AES depth profile of 2B-finished SUS 304 stainless steel exposed to the Shinomisaki marine site for 5 years (13)

2.4 Gel-like structure model and selected application

Based on the investigation of elemental distribution previously reviewed in section 2.3, one of the classic models of passive film formation was purposed. (5,6) The model was applied to explain the change of pitting potentials of stainless steel after exposure as reviewed in section 2.2.

Gel-like structure model was purposed in order to explain the effects of potential and aging time upon dry and wet corrosion based on the adsorption of bound water on surface film and the deprotonation process. Figure 2.14 shows a schematic sketch of the formation process of passive film by the successive deprotonation of water.

In Figure 2.14(a), bound water adsorbs on surface, and metal ions are produced by the anodic dissolution through an unprotected part on surface. It results in the formation of the intermediates denoted as MOH^+ . The deprotonation causes the losing of H^+ from H_2O . The process is further continuing to pull H^+ out from OH-M to be O-M as depicted in Figure 2.14 (b). This process can take place on other parts of surface, and the neighboring $\text{O-M-H}_2\text{O}$ are consequently bridged each other by H_2O as depicted in Figure 2.14(c). In the undeveloped part as shown in Figure 2.14 (d), intermediate compound MOH^+ can be produced and captured by surrounding H_2O resulting in the precipitation as solid film. The freshly formed film in this way still contains a lot of bound water. The anodic dissolution or the natural aging can be taken place accompanied by the dehydration. The structure of $\text{H}_2\text{O-M-OH}_2$ is progressively replaced by OH-M-OH , and then O-M-O depending on the degree of the proton loss.

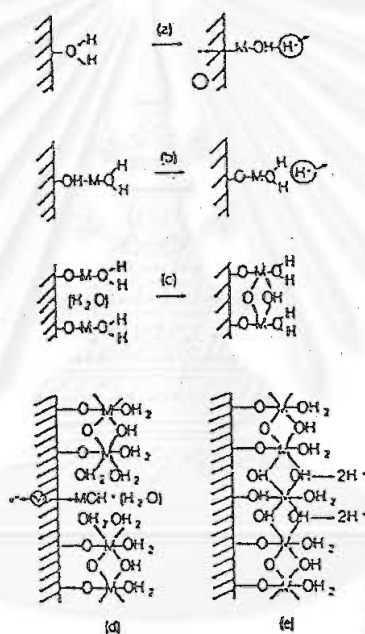


Figure 2.14 Schematic sketch of the process of the formation of passive film according to gel-like structure model (6)

As previously mentioned in section 2.2, pitting potentials reduced after the 2-year exposure period in the Milan urban-industrial site. N. Azzari (7) purposed that the degradation of passive film ensuing from the desorption of water molecules and adsorption of anions from the environment is very accentuated in the presence of chlorides, which can be found in urban-industrial site with other pollutants, such as sulphur dioxide. They accelerate the film dissolution. However, the reason for the increase in pitting potentials in the first 2-years period was not clearly explained. The desorption of water molecules and other anions were not proved by surface analysis methods especially at the points of the oxygen existence and the change of chemical states of oxygen in passive film. The existence and change of oxygen in the form of O^{2-} (H_2O), O^{2-} (OH^-) and O^{2-} (O) both before and after atmospheric exposure will be treated in the present work.

CHAPTER III

EXPERIMENTAL METHOD

3.1 History and installation for exposure test of specimens

Specimens in this study are 2B-finished SUS 304 and SUS 447J1 stainless steel sheets. They were produced by cold rolling, annealing and pickling. AES micrograph of 2B-finished surface of SUS 304 and SUS 447J1 are shown in Figure 3.1 and 3.2 respectively. Mass percent compositions of Cr, Ni, Mo, C, Si and Mn of both grades are reported in Table 3.1.

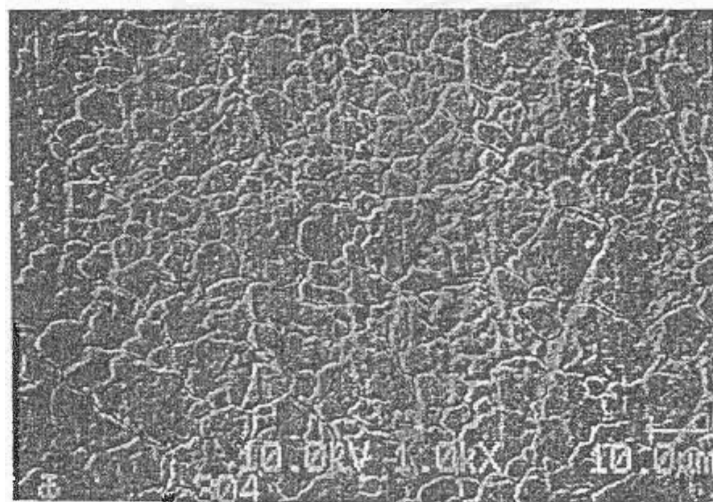


Figure 3.1 AES micrograph of 2B-finished SUS 304 stainless steel (As-received state).

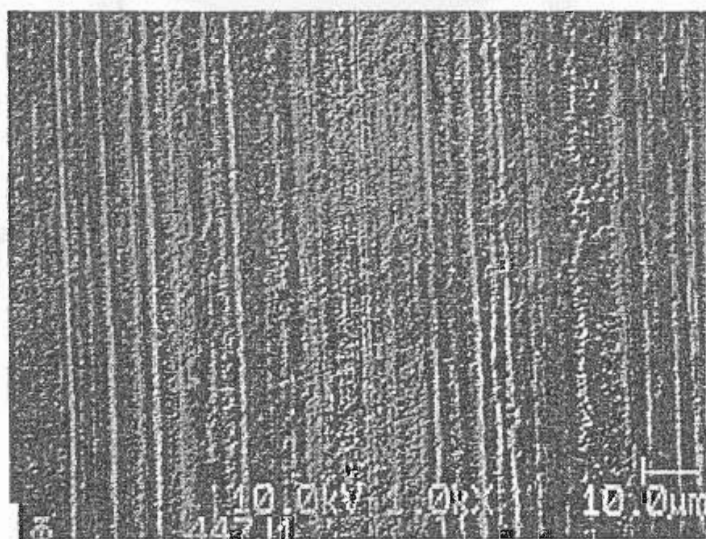


Figure 3.2 AES micrograph of 2B-finished SUS 447J1 stainless steel (As-received state)

Specimens were exposed to the Chiba urban-industrial site situated 1 km far from the seafront. Specimens with the dimension of 100cm x 150cm x 0.8cm(t) were fixed on the top surface of specimen holders inclined with the angle of 45° southward. The exposure period was carried out for 7 days in January 2001 and for 61 days during 22nd August to 22nd October 2000.

Table 3.1 Mass percent compositions of as-received SUS 304 and SUS 447J1 stainless steels

Steel	C	Si	Mn	P	S	Cr	Ni	Mo	N
SUS304	0.062	0.52	1.01	0.036	0.004	18.32	8.44	0.018	0.04
SUS447J1	0.005	0.19	0.13	0.021	0.004	29.76	0.16	1.91	0.012

3.2 Preparation of specimens

As for electrochemical measurements, specimens were cut to be a dimension of 2cm x 2cm x 0.8cm(t) without polishing. Then they were joined with steel wires. The shielding tape was wounded from the joint of specimen and wire to the rod far nearly 8 cm from the joint. The shielding polymer to remain the immersed area of 1cm x 1cm then covered the specimens. For XPS and AES analysis, specimens were cut to be the dimension of 1cm x 1cm x 0.8cm(t) without polishing. Ultrasonic cleaning and degreasing was done for 2 minutes before the measurement.

3.3 Experimental procedures

3.3.1 Measurement for pitting and corrosion potential

The 3.5-g/cm³ NaCl aqueous solution was used. It was maintained at 30°C for SUS 304 stainless steel and 70°C for SUS 447J1 stainless steel. Ag/AgCl reference electrode was applied and used as the reference for the report of pitting and corrosion potentials. The counter electrode was platinum type. The solution was first de-aerated by Ar gas bubbled in the solution for 30 minutes. The specimen was then immersed in, and Ar gas was changed to flow over the solution. The searching for corrosion potentials was done for 10 minutes. The current density was then detected as a function of the potentials. The anodic polarization started from the detected corrosion potentials with the scanning rate of 20 mV/min. The potentials at the current density of 10 $\mu\text{A}/\text{cm}^2$, $V \times 10$, were recorded as the index for the pitting potentials. The measurement procedure for corrosion potentials was as same as that for pitting potentials, but it was carried out at 30°C for both grades. The searching for corrosion potentials was done for 8 hours without the scanning for the anodic polarization.

3.3.2 AES analysis

The experiment was performed with the AES PHI model 595. Electron gun was operated at the acceleration voltages of 10 kV and the beam current of 1 μA . The ion gun was operated at the acceleration voltages of 2 kV and ion current densities of 20 $\mu\text{A}/\text{cm}^2$. Depth profiles of Fe, Cr, Ni, Mo, and O Auger electron intensities were derived by Argon sputtering for 30 seconds and proceeded by the detection of their

intensities alternately for 15 minutes. The sputtering rate estimated from the sputtering of pure iron was 2.1 nm/min.

3.3.3 XPS analysis

The instrument was performed with KRATOS AXIS HS. AlK α monochromatic x-ray contained the photon energy of 1486.6 eV was applied with the x-ray power of 15 kVx5mA. The incident angle of X-ray was 55° to the surface normal, whereas the take-off angle was 90°. The pass energy of 40 eV was used. The energy axis was horizontal shifted to set the binding energy of C1s at 284.6 eV. Shirley base line was drawn in order to quantify integrated peak intensity. Sensitivity factors of Fe, Cr and Ni accompanied by the accuracy of XPS measurement for stainless steel were evaluated through integrated peak intensities obtained from bulk stainless steel specimens. Relative sensitivity factors of Cr and Ni as well as the accuracy of the measurement of Fe and Cr Ni were obtained from the experiment according to appendix III. Relative sensitivity factors of Cr and Ni are 0.86 and 1.13 respectively, and that of O (1s) is 2.81. All relative sensitivity factors are normalized by that of Fe. Accuracies of the measurement of Fe and Cr are respectively 2.50 and 0.85 %.



สถาบันวิทยบริการ
จุฬาลงกรณ์มหาวิทยาลัย

CHAPTER IV

RESULTS AND DISCUSSION

The results concerning the influences of stainless steel grade and exposure period on pitting potentials, corrosion potentials, passive film thickness and chemical compositions-Cr, Ni, Mo and O- in passive film were firstly clarified. The results of the previous and the present works were discussed. The whole results obtained were then schematically integrated to depict the changes of passive film of SUS 304 and SUS 447J1 stainless steels after the 7- and 61-day exposure periods in the Chiba urban-industrial site. UV irradiation as the photo-inhibition of stainless steels immersed in aqua solution was finally stated in order to seek the common mechanism to the positive shift of pitting and corrosion potentials of SUS 304 and SUS 447J1 stainless steels in the atmospheric exposure, which exposed in the natural light UV irradiation.

4.1 Effects of stainless steel compositions and exposure periods on the pitting and corrosion potentials

The pitting potentials of SUS 304 and SUS 447J1 stainless steels exposed for 7 and 61 days in the Chiba urban-industrial site are illustrated in Figure 4.1 and 4.2 respectively.

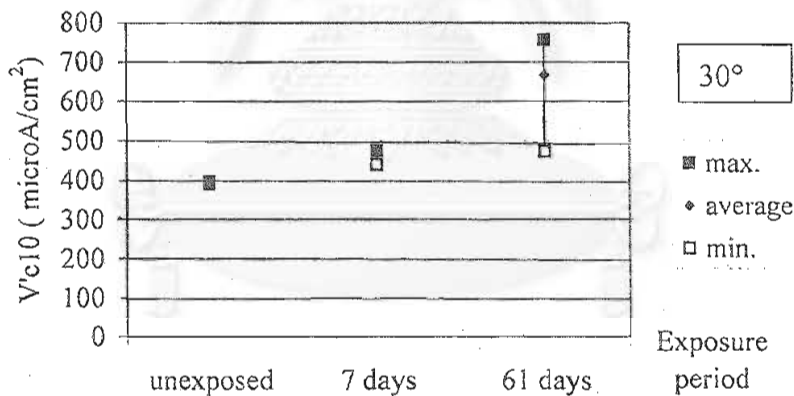


Figure 4.1 Pitting potentials of SUS 304 stainless steel exposed for 7 and 61 days in Chiba urban-industrial site

The temperatures of solution were maintained at 30 and 70°C for SUS 304 and SUS 447J1 stainless steels respectively. The measurement was repeated 3 times for each condition. One specimen was used for a measurement for one time. In the case of SUS 304 stainless steel as shown in Figure 4.1, an average pitting potential of the unexposed specimen is 394.3 mV_{Ag/AgCl}. It respectively increases to be 461.7 and 632 mV_{Ag/AgCl} after the exposure period of 7 and 61 days. In the case of SUS 447J1 stainless steel exhibited in Figure 4.2, the average pitting potential of unexposed specimen is 691 mV_{Ag/AgCl}. It respectively increases to be 881.7 and 965.3 mV_{Ag/AgCl} after the 7- and 61-day exposure periods.

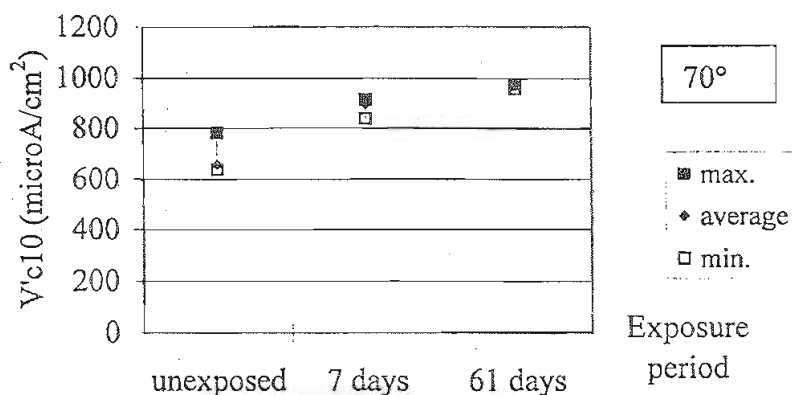


Figure 4.2 Pitting potentials of SUS 447J1 stainless steel exposed for 7 and 61 days in the Chiba urban-industrial site

It can be seen that pitting potentials of both grades after exposure are higher than those before exposure. Although the measurement for pitting potentials for SUS 447J1 stainless steel was carried out at the higher temperature than that for SUS 304 stainless steel, it still can be seen that pitting potentials of the as-received SUS 304 stainless steel is lower than those of SUS 447J1 stainless steel. And at the same exposure period, average-pitting potentials of SUS 447J1 stainless steel is higher than those of SUS 304 stainless steel.

As shown in Figure 2.2, Y. Kasawa reported the increase in pitting potential with the increase in Cr and Mo contents in model alloys. The present work investigated 2 types of stainless steels, which have different bulk chemical compositions of Cr and Mo. The Cr and Mo contents of SUS 447J1 stainless steel are respectively 29.76% and 1.91% and higher than Cr and Mo contents of SUS 304 stainless steel, which are 18.32% and 0.018% respectively. Even though the other alloying elements of these two grades are also different, especially Ni content that is 0.16% in SUS 447J1 stainless steel, but 8.44% in SUS 304 stainless steel, it still can be seen that pitting potentials of SUS 447J1 stainless steel, which contains high Cr and Mo contents, is higher than those of SUS 304 stainless steel. It was reported that Ni does not take part in passive film of SUS 304 stainless steel. (12) Then the effect of Ni on the promotion of corrosion resistance by taking part in passive film was questioned. In the present work the small amount of Ni was detected in the passive film of SUS 304 stainless steel and will be reported in section 4.3.2.

Corrosion potentials of the specimens unexposed and exposed for 7 days were measured and illustrated in Figure 4.3. The corrosion potentials of unexposed SUS 304 stainless steel were 161.3 mV_{Ag/AgCl} and increased to be 186 mV_{Ag/AgCl} after exposure for 7 days. In the case of unexposed SUS 447J1 stainless steel, it was 230 mV_{Ag/AgCl} and also increased to be 432 mV_{Ag/AgCl} after the 7-day exposure period. These evidences indicate that corrosion potentials of the as-received SUS 304 stainless steel are lower than those of SUS 447J1 stainless steel. At the same exposure period, corrosion potentials of both grades after exposure are higher than those before exposure.

As illustrating in Figure 2.4, N. Azzari also reported the increase in pitting potentials of SUS 304 stainless steel exposed in the first two year in the Milan urban-industrial site. The increase in corrosion potential as a function of exposure period was also reported as in Figure 2.3. Those and the present results are in agreed with for the case of SUS 304 stainless steel. The present work also confirms the increase in

pitting and corrosion potentials after atmospheric exposure for 7 and 61 days for SUS 447J1 stainless steel.

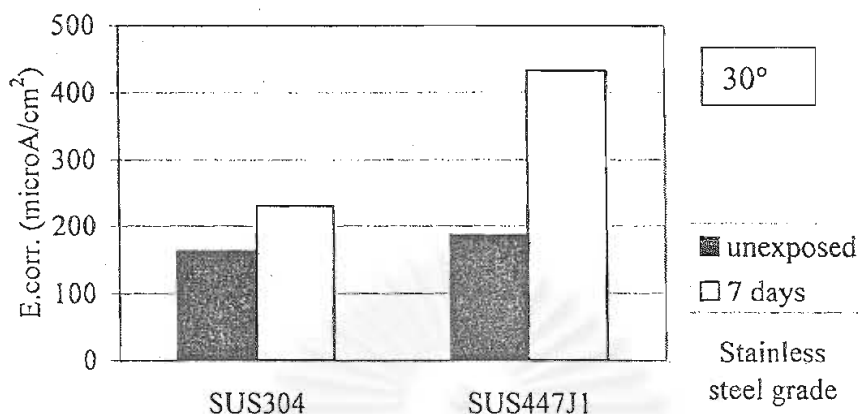


Figure 4.3 Corrosion potentials of SUS 304 and SUS 447J1 stainless steels unexposed and exposed for 7 days in the Chiba urban-industrial site

4.2 Effects of stainless steel compositions and exposure periods on the thickness of passive film

For the as-received SUS 304 stainless steel, Figure 4.4 illustrates the profile of Fe, O, Cr and Ni Auger electron intensity as a function of sputtering time. The sputtering times at the half of the maximum of O and Fe intensity were averaged to find out the estimate film thickness. The maximum intensity of Fe was selected at the intensity corresponding to the sputtering time of 9 minutes which the intensity of Fe was considered reaching the steady level. The sputtering rate in the case of pure iron, which is 2.2 nm/min, was applied to convert averaged sputtering time to the estimated passive film thickness.

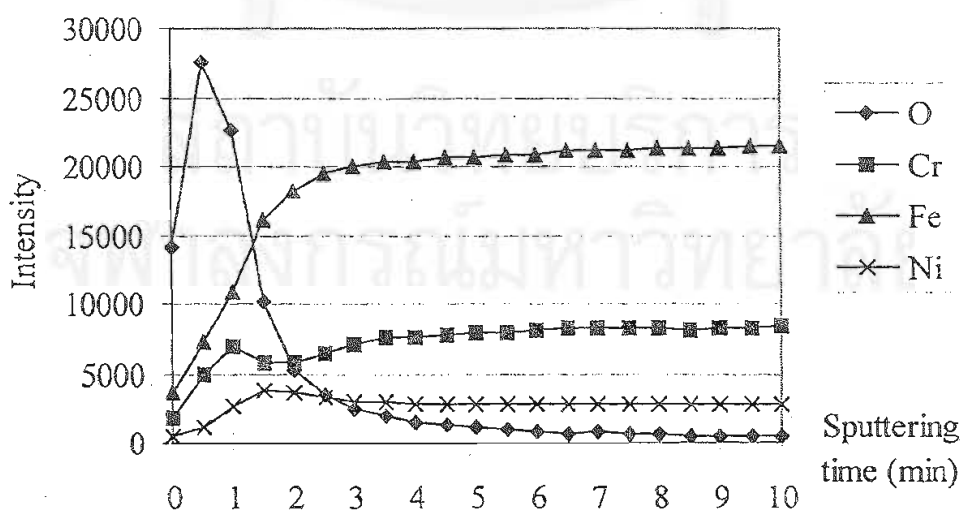


Figure 4.4 AES depth profile of Fe, O, Cr and Ni Auger electron intensity as a function of sputtering time of the as-received SUS 304 stainless steel

Figure 4.5 illustrates the Auger electron intensity emitting from oxygen in the compound form in passive film and substrate of SUS 304 and SUS 447J1 stainless steels. It is evident that passive film thickness of the as-received SUS 304 stainless steel is considerably more than that of SUS 447J1 stainless steel. By calculating the estimated film thickness by the previously described method, the estimated passive film thicknesses of SUS 304 and SUS 447J1 stainless steels are respectively 2.6 and 1.7 nm.

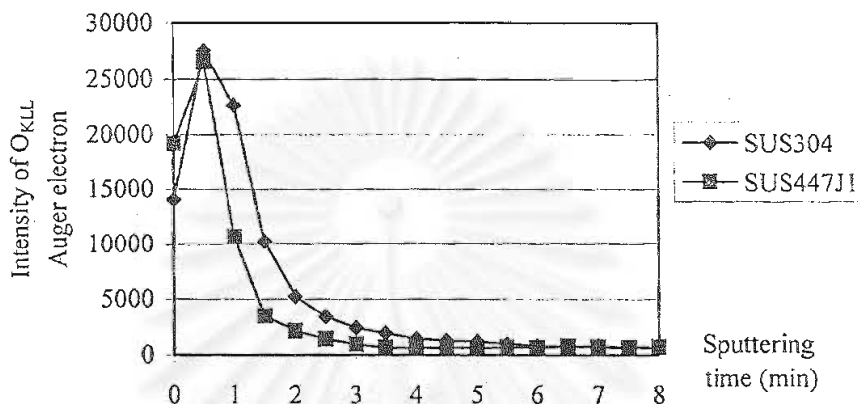


Figure 4.5 AES depth profile of O_{KLL} Auger electron intensity of the as-received SUS 304 and SUS 447J1 stainless steels as a function of sputtering time

As shown in Figure 2.6, it was reported by K. Asami, et. al. that film thickness of Fe-Cr alloy reduces when Cr content in bulk composition exceeds 13 atomic percent. It is also found in the present work that passive film thickness of SUS 447J1 stainless steel, which contains high Cr content compared to SUS 304 stainless steel, is less than that of SUS 304 stainless steel. Even though it cannot be directly compared with the previous study because the increase in Cr in the case of SUS 447J1 stainless steel is consistently accompanied by the change of amount of other alloying elements, such observation, however, should be noted.

The profile of O_{KLL} Auger electron intensity of SUS 304 stainless steel before and after exposure for 7 and 61 days in the Chiba urban-industrial site as a function of sputtering time was shown in Figure 4.6. The estimated film thicknesses of SUS 304 stainless steel were respectively 2.6, 1.6 and 2.2 nm before and after the 7-day and 61-day exposure period. The film thickness decreases after exposure. The film thickness of specimen exposed for 7 days is lower than that of specimen exposed for 61 days.

The profile of O_{KLL} Auger electron intensity of SUS 447J1 stainless steel after the 7- and 61-day exposure period in the Chiba urban-industrial site as a function of sputtering time is shown in Figure 4.7. The estimated film thicknesses are respectively 1.7, 1.6 and 1.9 nm for specimen unexposed and exposed for 7 and 61 days. It can be seen that the depth profile of O_{KLL} Auger electron intensity of specimens unexposed and exposed for 7 days are nearly the same. The depth profile of O_{KLL} Auger electron intensity of specimen exposed for 61 days could be considered no different to the unexposed and exposed 7-day specimens. It may be concluded that film thickness of SUS 447J1 stainless steel does not change considerably after exposure for 7 and 61 days in the Chiba urban-industrial site.

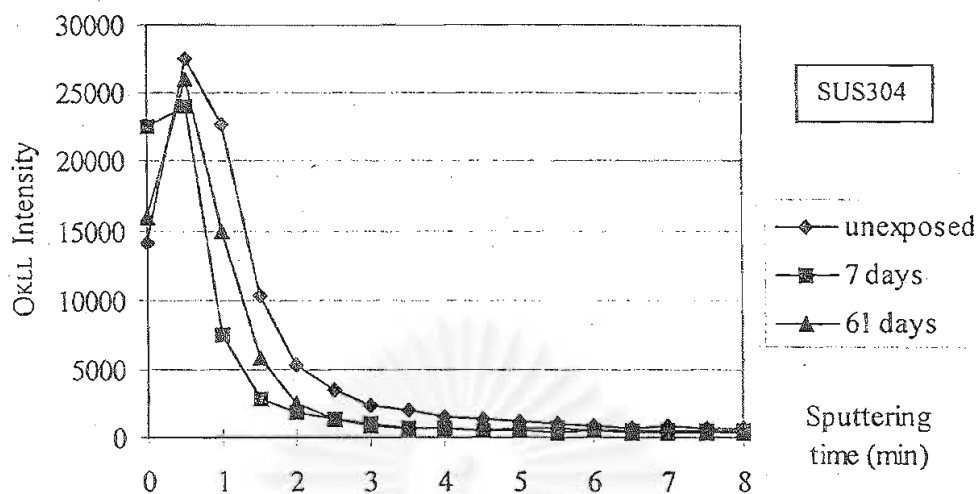


Figure 4.6 AES depth profile of O_{KLL} Auger electron intensity of SUS 304 stainless steel before and after exposure to the Chiba urban-industrial site for 7 and 61 days

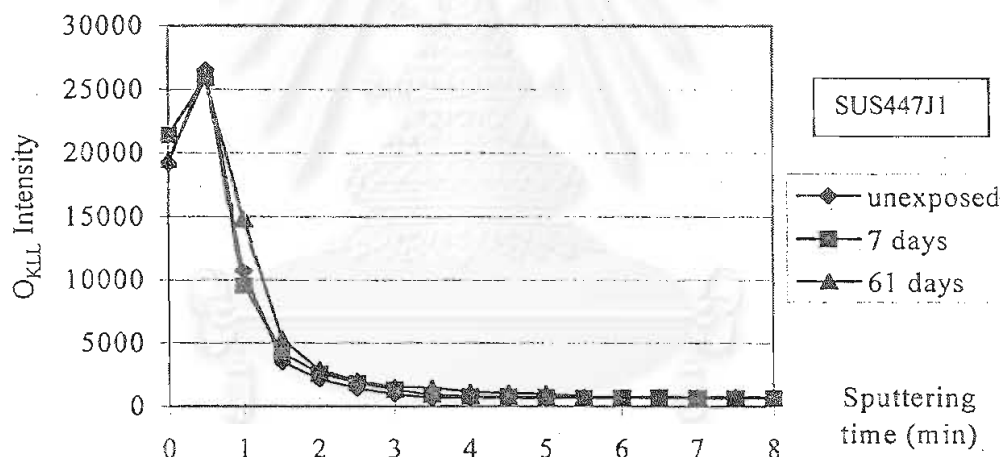


Figure 4.7 AES depth profile of O_{KLL} Auger electron intensity of SUS 447J1 stainless steel before and after exposed for 7 and 61 days in the Chiba urban-industrial site

As in Table 2.3, K. Asami, et al. reported the increase in passive film thickness of stainless steel after the 6-months exposure period in the Miyakojima subtropical and the Kinu-ura temperate site. M. Tochiara, however, confirmed the decrease in passive film thickness after the long-term exposure for 5 years in the Shionomisaki marine site as shown in Figure 2.13. For the short-term exposure for 7 and 61 days in the present work, the results of SUS 304 stainless steel indicated the decrease in passive film thickness after exposure. The inconsiderable change of passive film thickness of SUS 447J1 stainless steel was observed after the short-term exposure for 7 and 61 days in the Chiba urban-industrial atmospheric exposure.

4.3 Effects of stainless steel compositions and exposure periods on the composition of passive film

4.3.1 The Fe and Cr compositions

XPS spectra of $\text{Fe}2p_{3/2}$ and $\text{Cr}2p_{3/2}$ of as-received SUS 304 stainless steel are shown in Figure 4.8 and 4.9 respectively. The primary information of $\text{Fe}2p_{3/2}$ and $\text{Cr}2p_{3/2}$ spectra is the integrated peak intensity. It was obtained in the form of raw area constraint by a certain window of binding energy and bounded by peak intensity and base line. Background subtraction by drawing base line in the present work was in Shireley mode. XPS spectrum consists of the emitted photoelectron from both passive film and substrate. Photoelectron of metallic form, i.e. $\text{Fe}^0 2p_{3/2}$, $\text{Cr}^0 2p_{3/2}$ and $\text{Ni}^0 2p_{3/2}$, may emit from both passive film and substrate. In order to analyze composition in passive film, the subtraction of metallic peak intensity from the apparent peak was then applied. The binding energies of $\text{Fe}^0 2p_{3/2}$ and $\text{Cr}^0 2p_{3/2}$ are 706.8 eV and 574.1 eV respectively. (10) Integrated peak intensities were quantified to be atomic and finally weight percent under the consideration of the accuracy of the previously mentioned measurement. In this work, weight percent of Cr ion per Fe ion was used to indicate the degree of Cr enrichment.

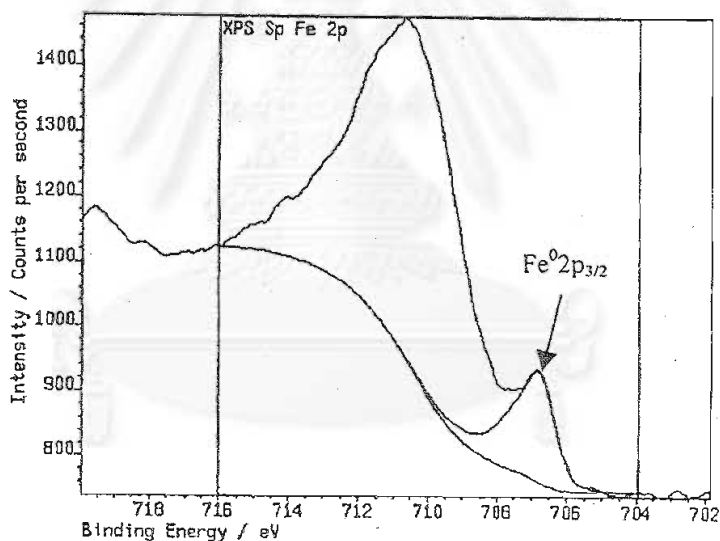


Figure 4.8 XPS spectrum of $\text{Fe}2p_{3/2}$ of as-received SUS 304 stainless steel

XPS spectra of $\text{O}1s$, $\text{Fe}2p_{3/2}$, $\text{Cr}2p_{3/2}$ and $\text{Ni}2p_{3/2}$ of SUS 304 stainless steel at different exposure periods are illustrated in Figure 4.10. Figure 4.11 depicts XPS spectra of $\text{O}1s$, $\text{Fe}2p_{3/2}$, $\text{Cr}2p_{3/2}$ and $\text{Mo}2d_{3/2,5/2}$ of SUS 447J1 stainless steel at different exposure periods. By calculating Cr enrichment according to the method described in appendix 2 using XPS spectra depicted in Figure 4.10 and 4.11, mass percent of Cr per that of Fe in passive film of as-received SUS 304 and SUS 447J1 stainless steels are then obtained as exhibited in Figure 4.12. Those values of as-received SUS 304 and SUS 447J1 stainless steels are 40.4% and 214.2%, respectively. From Table 3.1, mass percent of Cr per that of Fe in bulk of as-received SUS 304 and SUS 447J1 stainless steels are respectively 25.6 % and 44.1%. It then can be seen that Cr enrichment in passive film of as received SUS 304 and SUS 447J1

stainless steel. The increase in Cr enrichment from bulk to the outermost surface of SUS 447J1 stainless steel is markedly higher than that of SUS 304 stainless steel.

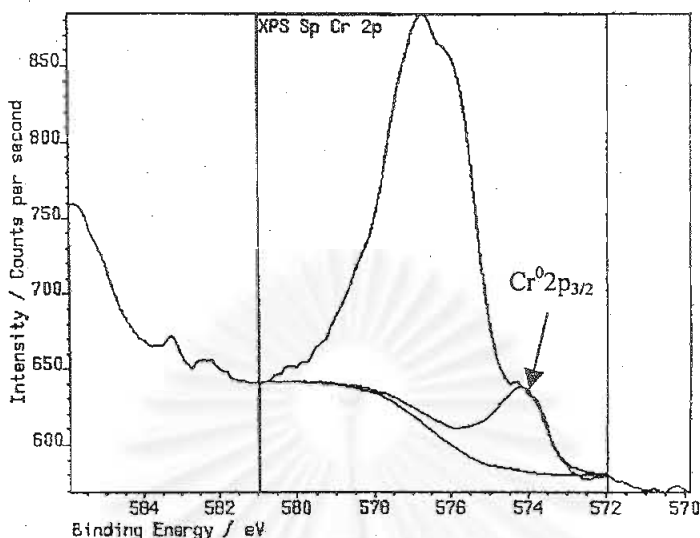


Figure 4.9 XPS spectrum of $\text{Cr}2p_{3/2}$ of as-received SUS 304 stainless steel

In the case of exposed SUS 304 stainless steel exhibited in Figure 4.12, the mass percents of Cr per those of Fe are 51.8 % and 81.3 % after the 7-day and 61-day exposure period respectively. By the accuracy of the measurement, it can be seen that Cr enrichment considerably increases with the increased exposure period. Cr enrichment of specimen exposed for 61 days is higher than that exposed for 7 days. In the case of SUS 447J1 stainless steel shown in the same Figure, the mass percents of Cr per those of Fe are respectively 198.2 % and 236.3% after the 7-day and 61-day exposure period. The analytical data are in the ranges of 193.2% to 239.4%, 178.9% to 221.3% and 221.6% to 266.6% for specimens unexposed and exposed for 7 days and 61 days respectively. By the accuracy of measurement, it cannot be considered that the changes of Cr enrichment are distinguished in the case of SUS 447J1 stainless steel exposed 7- and 61-day in the Chiba urban-industrial site.

As reviewed in section 2.3.2, K. Asami, et al. investigated passive films of various stainless steels exposed in atmosphere. The averaged cationic fraction of SUS 304 and SUS 316 stainless steels passive film after exposure at different site depicts in Figure 2.11. For SUS 430 and SUS 444 stainless steels, it is illustrated in Figure 2.12. It can be seen that Cr diminishes after exposure. M. Tochiara, however, reported the enrichment of Cr in the passive film after the long-term exposure as shown in Figure 2.13. In the present work, the results show the trends of Cr enrichment after exposure in the case of SUS 304 stainless steel but the indistinguishable change in Cr enrichment in the passive film is observed in the case of SUS 447J1 stainless steel.

From the results of SUS 447J1 stainless steel, the pitting and corrosion potentials increase after exposure, but the considerable change in passive film thickness and Cr enrichment cannot be observed. The question is what affects or relates to the positive shift of pitting and corrosion potentials? The further inquiry will be done in the next sections.

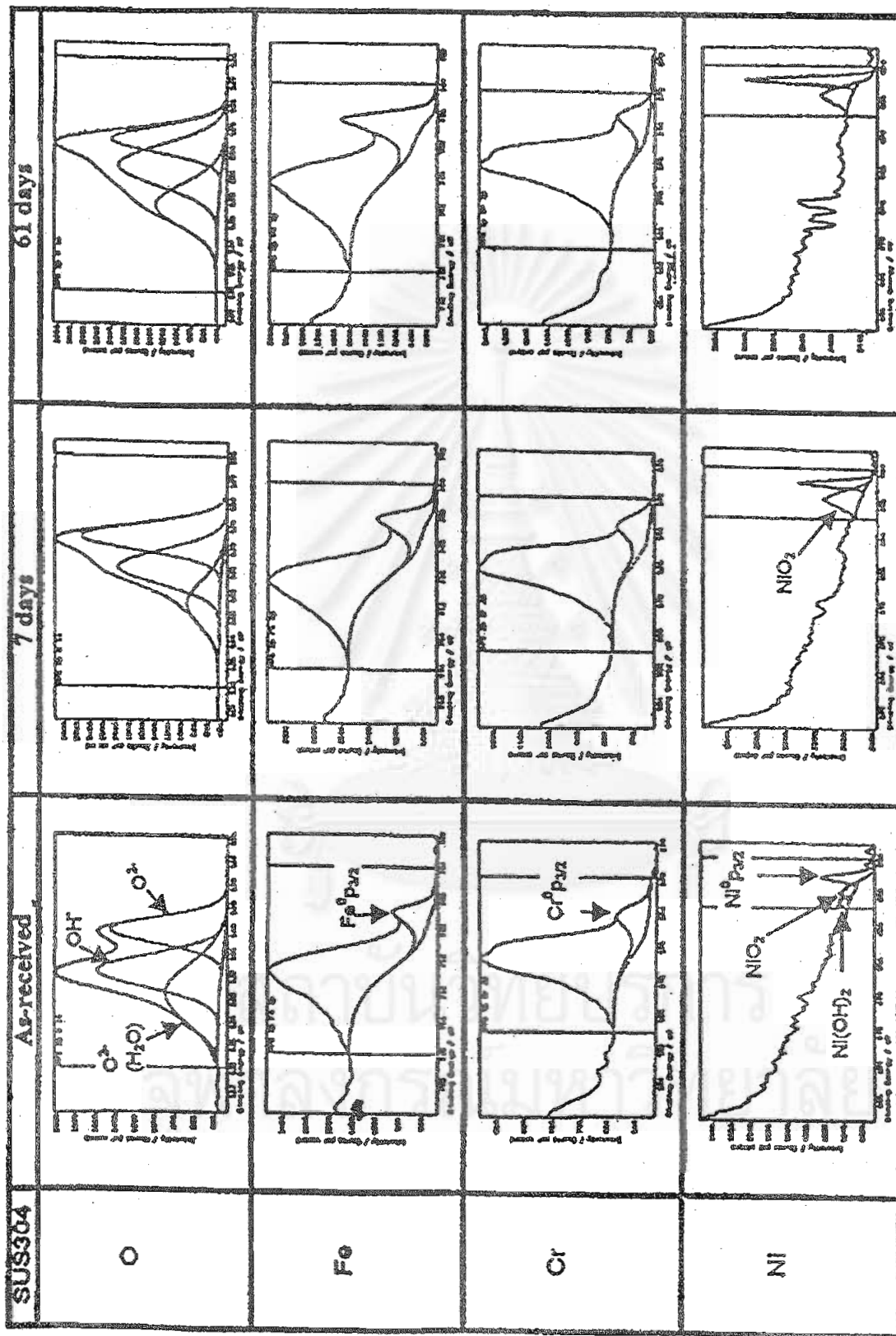


Figure 4.10 XPS spectra of O1s, Fe2p_{3/2}, Cr2p_{3/2}, and Ni2p_{3/2} of SUS 304 at different exposure periods

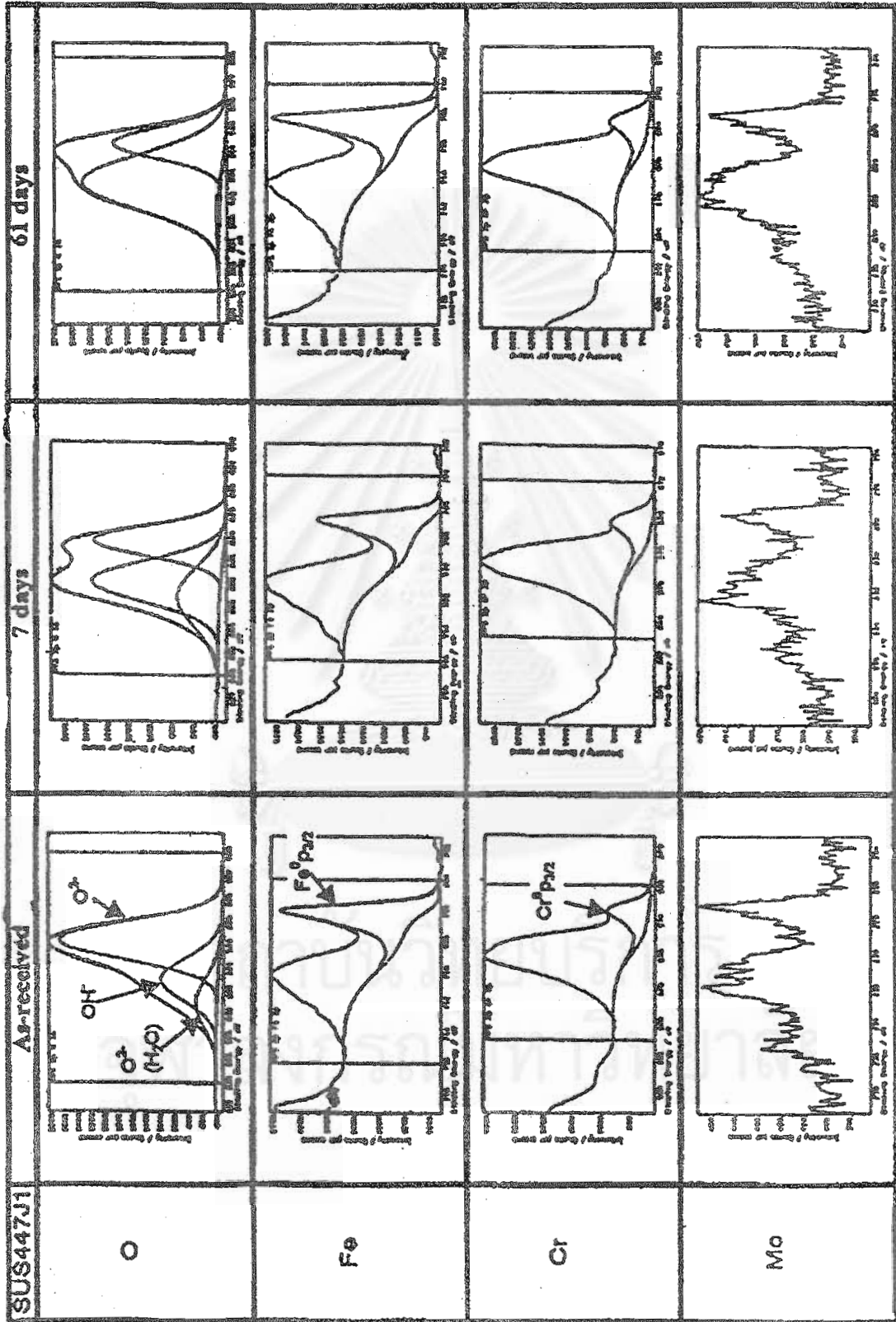


Figure 4.11 XPS spectra of O1s, Fe2p_{3/2}, Cr2p_{3/2}, and Mo2d of SUS 447J1 at different exposure periods

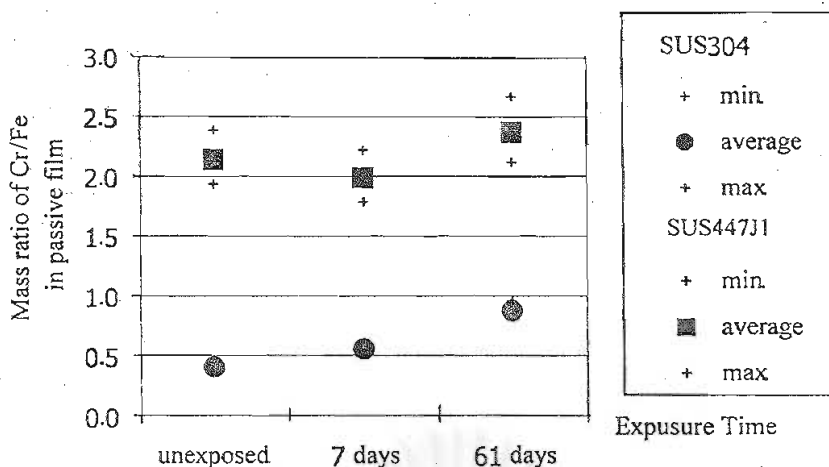


Figure 4.12 Cr enrichments in passive films of SUS 304 and SUS 447J1 stainless steels at different exposure periods

4.3.2 The Ni and Mo compositions

From Table 3.1, SUS 304 stainless steel contains 18.32 wt-% Cr, 8.44 wt-% Ni and SUS 447J1 stainless steel contains 29.76 wt-% Cr, 1.91 wt-% Mo. The elemental distributions of Ni and Mo were then successively investigated for SUS 304 and SUS 447J1 respectively.

Figure 4.13 shows XPS spectra of Ni $2p_{3/2}$ of as-received SUS 304 stainless steel. Ni peak was deconvoluted to be three peaks. They are Ni metallic (Ni $^{0}2p_{3/2}$), nickel oxide (NiO) and nickel hydroxide (Ni(OH) $_2$) peaks. The binding energies are respectively 852.9 eV (10), 854-855 eV and 856-856.5 eV (19).

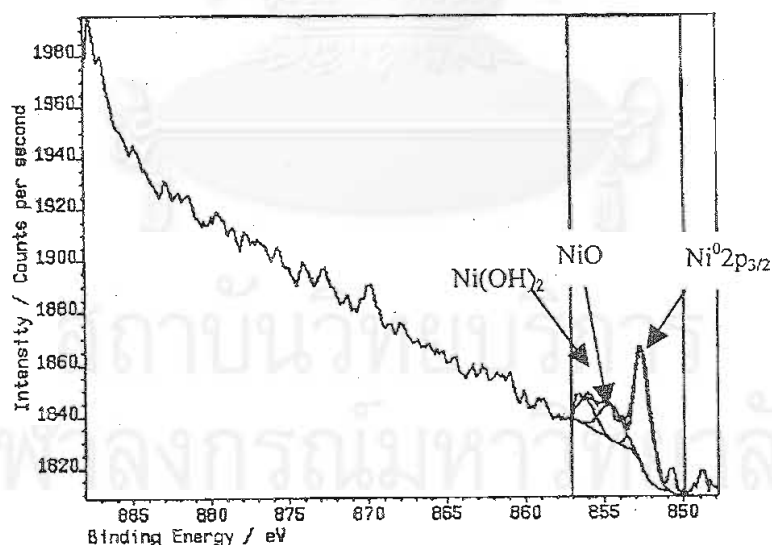


Figure 4.13 XPS spectrum of Ni $2p_{3/2}$ of as-received SUS 304 stainless steel

In the passive film of SUS 304 stainless steel, both nickel oxide and hydroxide were slightly observed in unexposed specimens. However, only oxide film can be observed after the 7-day and 61-day exposure periods in the Chiba urban-industrial site. It is possible that nickel hydroxide in passive film of unexposed specimen was deprotonized and changed to be nickel oxide after the 7-day exposure. In Figure 4.14, mass ratios of Ni/Fe-Cr-Ni in the compound formed in passive film after different

exposures are 1.4%, 3.2% and 2.3%. It can be seen that, even though Ni was added 8.44% in bulk composition, but it slightly took part in passive film, which was 1.4% in the unexposed specimen. After specimens were exposed for 7 days and 61 days, passive film thickness decrease as in figure 4.6.

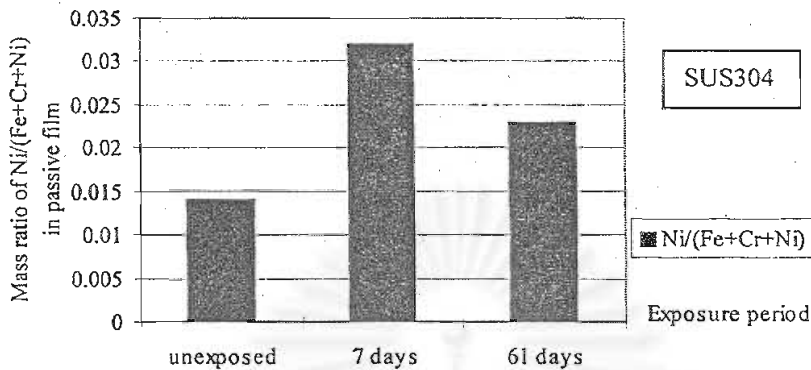


Figure 4.14 Ni enrichments in passive films of SUS 304 stainless steel after different exposure periods

Based on the assumption that the density of passive film in each condition is not different markedly, it may consider that the passive film thickness decrease due to the reductions of passive film volume and mass. If the Ni content of compounds in the passive film was considered nearly constant and the passive film mass decrease after exposure, the increases of Ni mass percent in the passive film was observed. This is reflected in Figure 4.14. The film thickness of specimen exposed for 7 days is less than that exposed for 61 days. It appears that mass percent of Ni in passive film change considerably after exposure. The specimen exposed for 7 days has higher nickel mass percent than that unexposed and exposed for 61 days.

The integrated peak intensity of Mo in passive film of as-received SUS 447J1 stainless steel, and after different exposure periods is showed in Figure 4.15 and 4.11 respectively. The binding energies of Mo at the oxidation states of 0, +4 both oxide and hydroxide form and +6 for oxide form are in the ranges from 227.8 to 235.6 eV. (10) However, it shows that the spectra have severely the noise effect. Subsequently, the considerable change of Mo peak cannot be clearly investigated for the specimens exposed for 7 and 61 days.

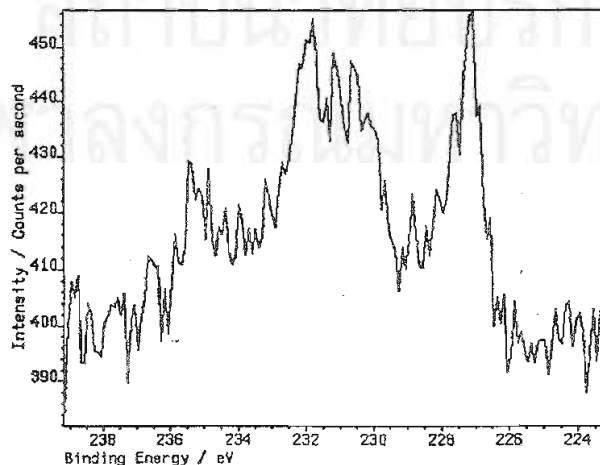


Figure 4.15 XPS spectra of Mo $2d_{3/2,5/2}$ of as-received SUS 447J1 stainless steel

4.3.3 The oxygen distribution

The O1s spectrum of as-received SUS 304 stainless steel is depicted in Figure 4.16. It was deconvoluted to be 3 peaks. They are O^{2-} , OH^- and bound water (H_2O). The binding energies are respectively 529.9-530.3 eV, 531.6 eV and 532.6 eV. (10)

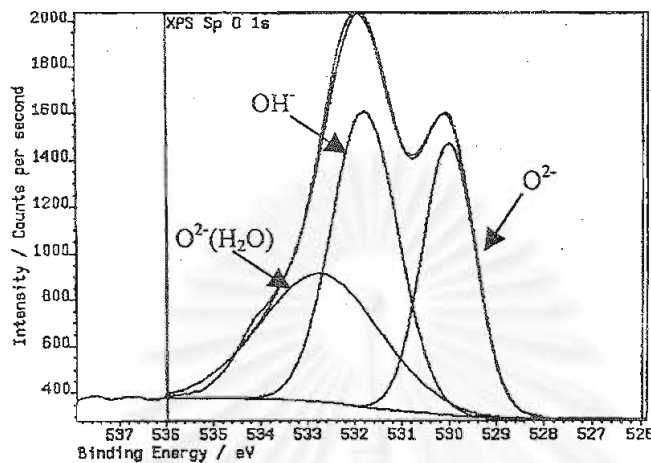


Figure 4.16 O1s spectrum of as-received SUS 304 stainless steel

In order to investigate the shift of O1s XPS spectrum with the exposure period, the photoelectron intensities of OH^- and H_2O were grouped and compared to the photoelectron intensity of O^{2-} for SUS 304 stainless steel. The photoelectron intensities of OH^- and H_2O per O^{2-} are shown in Figure 4.17. The ratio is 2.42 for unexposed condition. It indicates that the photoelectron intensity of OH^- and H_2O is higher than that of O^{2-} . This ratio reduces to 1.34 after the 7-day exposure period, but is nearly constant (2.41) after the 61-day exposure period. If the successive evaluation could be applied, it may say that O1s shifts to the decrease in OH^- and H_2O spectra after the 7-day exposure. This ratio, however, reversibly shifts to the increase in OH^- and H_2O spectra after specimen was exposed for 61 days. The change in this ratio will be discussed with the change in passive film thickness in the next section.

It should be mentioned here that the specimens were exposed to the different atmospheres. The environmental effect may be included in the results.

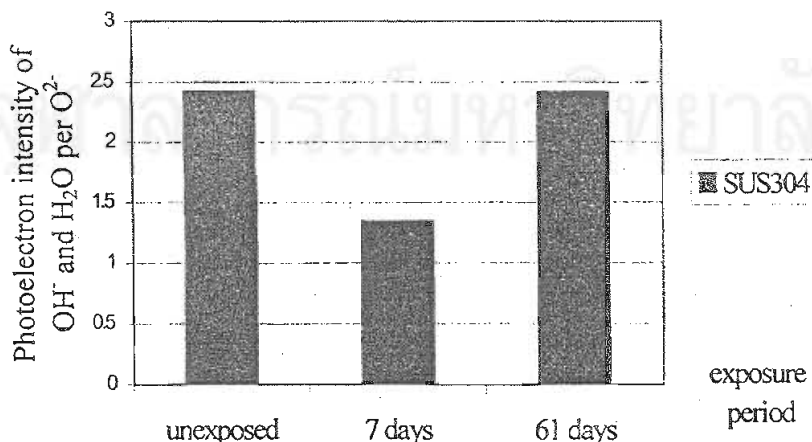


Figure 4.17 The photoelectron intensity of OH^- and H_2O per O^{2-} of SUS 304 stainless steel at the different exposure periods

In the case of SUS 447J1 stainless steel exposed for 7 days, the photoelectron intensities of H_2O per OH^- , H_2O and O^{2-} , of OH^- per OH^- , H_2O and O^{2-} , and of O^{2-} per OH^- , H_2O and O^{2-} were calculated by using deconvoluted peaks of O1s shown in figure 4.10 and 4.11. The photoelectron intensities of H_2O per OH^- , H_2O and O^{2-} increase from 0.11 for unexposed specimen to 0.2 for specimen exposed for 7 days in snowy winter in the Chiba urban-industrial site. It is believed that such environment contained higher relative humidity than specimen unexposed and exposed for 61 days, which was held in Summer. Then the increase of H_2O layer causing by the water adsorption from atmosphere was observed. In Figure 4.18, the photoelectron intensities of OH^- per OH^- , H_2O and O^{2-} increase from 0.25 for unexposed specimen to 0.46 for specimen exposed for 7 days. The photoelectron intensities of O^{2-} per OH^- , H_2O and O^{2-} decrease from 0.64 for unexposed specimen to 0.34 for specimen exposed for 7 days. It is then possible that H_2O were deprotonized and changed to be OH^- , and the H^+ from such process was captured by O^{2-} resulting in OH^- . Finally, it results in the decrease in H_2O and O^{2-} as well as the increase in OH^- in passive film.

In the case of SUS 447J1 stainless steel exposed for 61 days, the photoelectron intensities of H_2O per OH^- , H_2O and O^{2-} decrease from 0.11 for unexposed specimen to 0.02 for specimen exposed for 61 days in Summer. Similar as above discussion, it is believed that the atmosphere in Summer contained lower relative humidity than that for unexposed and 7-day exposed specimens, which were held in Winter. Then the increase in H_2O layer causing by the water adsorption from atmosphere may be less than the cases of unexposure and the 7-day exposure. Additionally, the effect of temperature in Summer may increase the kinetics of deprotonation of H_2O to be OH^- or O^{2-} resulting in the drastic reduction of H_2O . However, it is still found that the photoelectron intensities of OH^- per OH^- , H_2O and O^{2-} increase from 0.25 for unexposed specimen to 0.67 for specimen exposed for 61 days as in Figure 4.18. And the photoelectron intensities of O^{2-} per OH^- , H_2O and O^{2-} decrease from 0.64 for unexposed specimen to 0.31 for specimen exposed for 61 days. It is possible, as same as the former case, that H_2O were deprotonized and changed to be OH^- , and the H^+ from such process will be captured by O^{2-} resulting in OH^- . It then results in the decrease in H_2O and O^{2-} as well as the increase in OH^- in passive film.

From the result, the increase in hydroxide, OH^- , films took places for those two conditions. This change will be further discussed with the previous results in the next section.

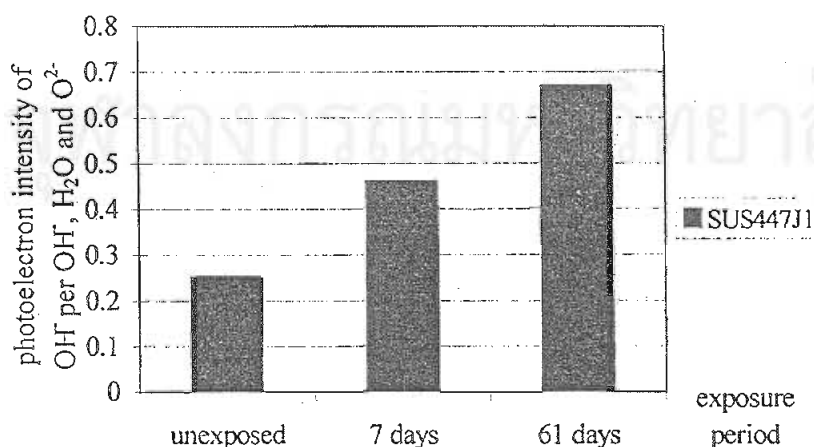


Figure 4.18 The photoelectron intensity ratios of OH^- per OH^- , H_2O and O^{2-} of SUS 447J1 stainless steel at the different exposure periods

4.4 Schematic sketch of the change in construction of passive film of SUS 304 and SUS 447J1 stainless steels before and after atmospheric exposure for 7 days and 61 days

The schematic sketches of SUS 304 and SUS 447J1 stainless steels passive films before and after exposures for 7 and 61 days in the Chiba urban-industrial site are depicted in Figure 4.19. Cr and Fe in the compounds formed in passive film were considered. The horizontal dot line is used to indicate the hydroxide and oxide layers. In this sketch, hydroxide means OH^- and H_2O in passive film.

In the case of SUS 304 stainless steel exposed for 7 days, it is possible that Fe cation in passive film was dissolved from passive film to atmosphere after exposure. It then resulted in the increase in Cr enrichment. Many works reviewed as depicted in Figure 2.8 to 2.10 exhibited the covering of hydroxide layer on the top surface of passive film. As in Figure 4.17, the decrease in photoelectron intensity of OH^- and H_2O per O^{2-} in passive film in the 7-day exposure in the case of SUS 304 stainless steel was observed. It is then possible that OH^- and H_2O film, at least that formed on as-received specimen, was removed from passive film to atmosphere. The dissolution of both Fe cation and the removing of OH^- and H_2O film may result in the decrease in thickness of passive film.

In the case of SUS 304 stainless steel exposed for 61 days, it is considered that Fe cation in passive film was dissolved from passive film to atmosphere after exposure resulting in the increase in Cr enrichment. It may also consider that hydroxide film, at least that formed on as-received specimen, and Fe cation, as previously mentioned, were removed from passive film to atmosphere resulting in the decrease in thickness of passive film. However, it appears that film thickness reduces after exposure, but the photoelectron intensities of OH^- and H_2O per O^{2-} are nearly constant. It is then considered that oxide in passive film was changed to be hydroxide in passive film in order to maintained this ratio.

The successive evaluation of passive film with the exposure period is limited by the different seasons between specimens exposed for 7 and 61 days. However, if it is considered that the 7-day exposure period represents the early condition of the atmospheric exposure, then the additional phenomena can be discussed. OH^- and H_2O film is considered that it was removed from passive film after the exposure period of 7 days as previously discussed. However, it appears that passive film thickness and the photoelectron intensities of OH^- and H_2O per that of O^{2-} in passive film after the 61-day exposure period were more than those of specimen exposed for 7 days. It is then considered that new OH^- and H_2O film grows after the exposure. The passive film of specimen exposed for 61 days is not severely removed as same as that of specimen exposed for 7 days. It seems that hydroxide film formed after exposure is tougher than hydroxide film formed on as-received specimen. From the previous discussion, it is suggested that OH^- and H_2O film formed after exposure can be occurred by 2 possibilities. The first is the transformation of oxide in passive film to be hydroxide in passive film. The second is the growth of H_2O or OH^- film after exposure. The thickness of OH^- and H_2O film after exposure as well as pitting and corrosion potentials increase. For the case of SUS 304 stainless steel, Cr enrichment and OH^- and H_2O film formed after exposure are considered the cause of the increase in pitting and corrosion potentials.

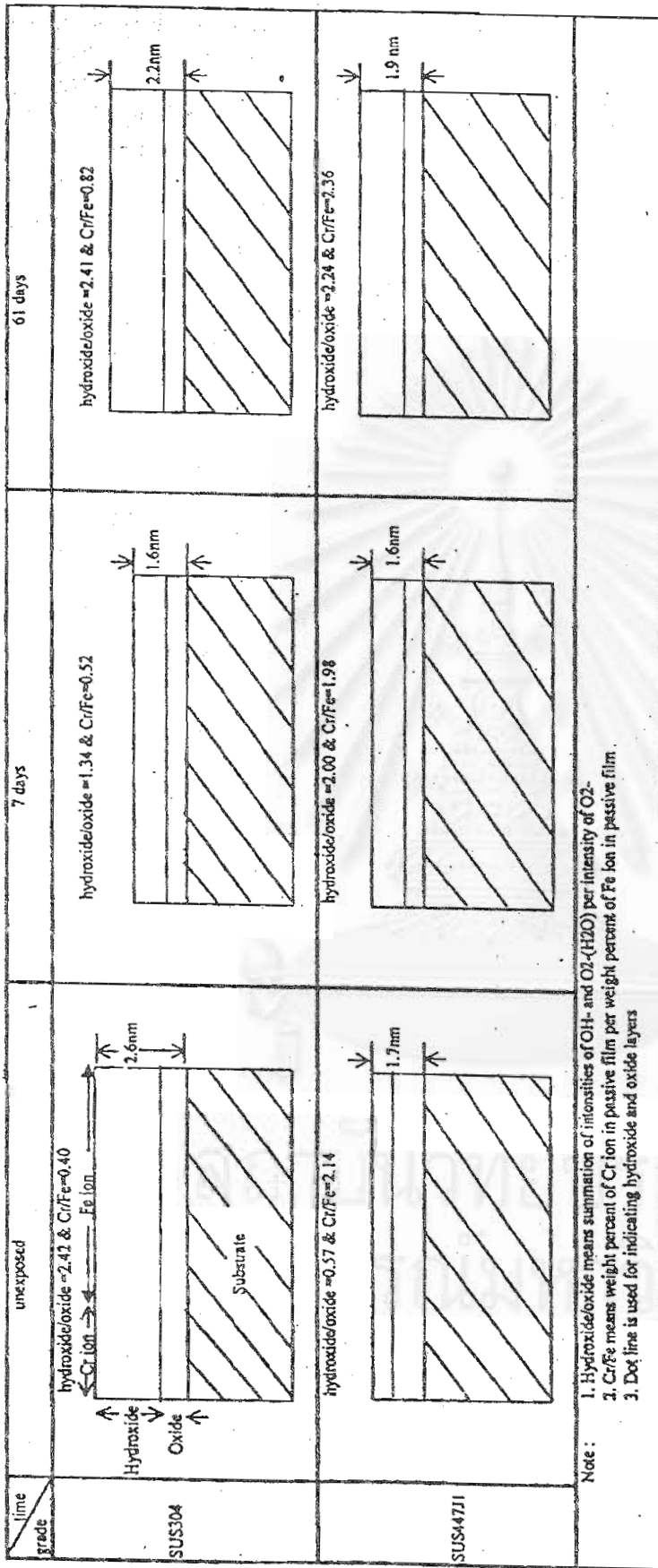


Figure 4.19: Schematic sketch of the change in construction of passive film of SUS 304 and SUS447J1 stainless steels

In the case of SUS 447J1 stainless steel, it appears that pitting and corrosion potentials of SUS 447J1 stainless steel increase after exposure, but the considerable change of passive film thickness and Cr enrichment cannot be observed. The change of Mo content may affect the pitting and corrosion potentials, but it cannot be analyzed in the present work. It is purposed that, at least, hydroxide formed after exposure plays the role on the positive shift of pitting and corrosion potentials.

By comparing SUS 304 and SUS 447J1 stainless steels, it can be seen that after exposure, pitting and corrosion potentials of the both grades increase. At the same exposure period, pitting and corrosion potentials of SUS 447J1 stainless steel are higher than those of SUS 304 stainless steel. The different and common possible mechanism was here purposed. In the case of SUS 304 stainless steel, after exposure film thickness reduces, but Cr enriches, and the new OH⁻ and H₂O film was formed. The Cr enrichment and the formation of OH⁻ and H₂O film after exposure were considered to be the cause of positive shift of pitting and corrosion potentials. However, in the case of SUS 447J1 stainless steel, the considerable changes of passive film thickness cannot be found, especially for specimen unexposed and exposed for 7 days that the AES depth profiles are nearly the same path. It is then considered that passive film of SUS 447J1 stainless steel has more resistant to be removed by environment, or tougher than that of SUS 304 stainless steel. Cr enrichment of as-received SUS 447J1 stainless steel is higher than that of SUS 304 stainless steel. After exposure, the change of Cr enrichment in passive film of SUS 447J1 stainless steel cannot be clearly found, whereas it considerably increases in the case of SUS 304 stainless steel. Nevertheless, at the same exposure period, Cr enrichment in passive film of SUS 447J1 stainless steel is higher than that of SUS 304 stainless steel. The increase in hydroxide in passive film of SUS 447J1 stainless steel can be observed and was considered that it relates to the increase in pitting and corrosion potentials.

4.5 Photo-inhibition under UV and natural light irradiation

Specimen atmospherically exposed is considered that it is also affected by the natural light irradiation. The photo-inhibition, the increase in pitting potential of specimen subjected to UV irradiation, was also observed in various laboratories that included the case of stainless steels. (20-22) The photo-quenching of electric field strength in passive film was first purposed based on point defect model. This model purposes that the passivity breakdown occurs when the accumulation rate of cationic vacancies at substrate/film interface is critically more than the rate that cationic vacancies can be annihilated at the same interface. (20,21,23) In the case of photo-inhibition of passivity breakdown, it was purposed (20,21) that incident photons that contain energies more than the bandgap energy of passive film generate electron-hole pairs. They are then separated by the steep potential gradient in the manner to quench, or reduce, the electric field strength in passive film. The reduction of electric field decreases the flux of cationic vacancies that transport from film/solution interface across passive film to substrate/film interface. The decrease in the flux of cationic vacancy then promotes the increase in the breakdown potential. The modification of vacancy structure after stainless steel is subjected to UV irradiation was also purposed. The photo-inhibition caused by this mechanism that can be persisted after UV irradiation is removed over the relaxation time. The recent work (23) also reported the Cr enrichment after SUS 304 subjected to UV irradiation. The Cr enrichment of SUS 304 stainless steels under UV irradiation may increase the pitting

potential. The photo quenching of electric field in passive film and Cr enrichment were the possible causes of the photo-inhibition under the UV irradiation. However, the ultimate solution for the mechanism of this phenomenon is still in consideration.

The present work investigated the transformation of passive film in the atmospheric exposure. The natural light irradiation may be a factor that affects the transformation of passive film. Although the passive film that atmospherically exposed should be different from the passive film that exposed under the controlled condition of UV irradiation in laboratory, but the Cr enrichment can be observed in cases for SUS 304 stainless steel. In this work, the role of hydroxide formed after exposure, and may also be formed because of the natural light irradiation, on the positive shift of pitting and corrosion potentials was also suggested. The result can be observed in the case of SUS 447J1 after the exposure period of 7 days. However, the further experimental work should be conducted to confirm the results.



สถาบันวิทยบริการ
วาลงกรณ์มหาวิทยาลัย

CHAPTER V

CONCLUSIONS

The 2B-finished SUS 304 and SUS 447J1 stainless steels were atmospherically exposed for 7 and 61 days in the Chiba urban-industrial site, then electrochemical measurements accompanied by XPS and AES analysis were carried out in order to investigate passive films. The following conclusions can be drawn,

1. The as-received SUS 304 stainless steel has lower chromium enrichment in passive film as well as lower pitting and corrosion potentials, but thicker passive film than the as-received SUS 447J1 stainless steel.

2. The pitting potentials as well as corrosion potentials of SUS 304 and SUS 447J1 stainless steels increase after exposure. At the same exposure period, pitting and corrosion potentials of SUS 447J1 stainless steel are more than those of SUS 304 stainless steel.

3. After exposure, Cr enrichment in passive film increases, Ni content in passive film seems exhibiting no change, and film thickness reduces in the case of SUS 304 stainless steel. Cr enrichment and film thickness are not distinguished in the case of SUS 447J1 stainless steel.

4. After exposure, the photoelectron intensity ratio of OH^- and OH_2 per that of O^{2-} reduces after the 7-day exposure period and is nearly constant after the exposure period of 61 days in the case of SUS 304 stainless steel. The photoelectron intensity ratio of OH^- per OH^- , OH_2 and O^{2-} increases after exposure for 7 days and 61 days in the case of SUS 447J1 stainless steel.

5. In the case of SUS 304 stainless steel, Cr enrichment and hydroxide film formed after exposure are considered to increase the pitting and corrosion potentials. In the case of SUS 447J1 stainless steel, hydroxide film formed after exposure is considered to increase the pitting and corrosion potentials.

สถาบันวิทยบริการ
จุฬาลงกรณ์มหาวิทยาลัย

REFERENCES

1. Kawasaki, Tasuo. *Kawasaki Steel Technical Report* 40 (May 1999): 5-15.
2. Oka, Yutaka, and Noriyuki Kuriyama. *Kawasaki Steel Technical Report* 40 (May 1999): 36-38.
3. Kasawa, Yoshihiro, Keiichi Yochioka, and Fusao Togashi. *Kawasaki Steel Technical Report*, 31 (November 1994): 35-43.
4. Tochiwara, Misako, Takumi Ujio, Yoshihiro Kasawa and Susumu Satoh. *Materials Performance* (December 1996): 58-62.
5. Okamoto, G., and T. Shibata. Passivity and the Breakdown of Passivity of Stainless Steel. In Robert P. Frankenthal and Jerome Kruger (eds.), *Passivity of Metal*, Princeton, New Jersey: The Electrochemical Society, 1978.
6. Lacombe, P., B. Baroux and G. Baranger (eds.), *Stainless Steel*, Translated by Jame H. Davidson and John B. Lindquist. France: Les Editions de Physique, 1993.
7. Azzari, Nazzareno. *Corrosion Science* Vol.12, 9 (1982): 867-876.
8. Asami, K., and K. Hashimoto. *Proc. 13th Int. Corrs. Congr.*, 1 (1996): 219-226.
9. Olefjord, I., and L. Wegrelius. *Corrosion Science* 31 (1990): 89-98.
10. Vito, E. De, and P. Marcus. *Surface and Interface Analysis* 19 (1992): 403-408.
11. Sarit Chaikittisilp, *Master's Thesis*, department of Metallurgical Engineering, Faculty of Engineering, Chulalongkorn University, Thailand, 2000.
12. G. Lothogkum, A. Klinkeson and P. Jivavibul, *Proc. 14th Int. Corrs. Congr., Cape town, South Africa, 1999*, pp.531-538. Cape town, South Africa, 1999.
13. Tochiwara, Misako, et. al. *CAMP-ISIJ* 13 (2000): 633.
14. Sedricks, A. John. *Corrosion of Stainless Steel*. USA.: John Wiley & Sons, 1996.
15. Kasawa, Yoshihiro. *private communication*.
16. Asami, K., K. Hashimoto, and S. Shimodaira. *Corrosion Science* 18 (1978): 151-160.
17. Asami, K., K. Hashimoto, and S. Shimodaira. *Corrosion Science* 18 (1977): 713-723.
18. Salmon, Richard. *Alloy and oxide analysis by XPS method*, unpublished document, 1998.
19. Physical electronics. *Handbook of XPS spectroscopy*.
20. Macdonald, D.D., E. Sikora, M.W. Balmas and R.C. Alkire. *Corrosion Science* Vol.38, 1 (1996): 97-103.
21. Breslin, Carmel B., Dugdy D. Macdonald, Elzbieta Sikora and Janusz Sikora. *Electrochimica Acta*, Vol.42, 1 (1997): 137-144.
22. Fujimoto, S., T. Yamada, and T. Shibata. *Journal of Electrochemical Society* Vol. 145, 5 (May 1998): L79-L81.
23. Mcdonald, D.D. *Journal of Electrochemical Society* Vol. 139,12 (December 1992): 3434-3449.
24. Briggs. D., and M.P. Seah. *Practical Surface Analysis Volume 2: Auger and X-ray Photoelectron Spectroscopy*. United Kingdom: John Wiley & Sons, 1990.

25. Ikeo, N., Y. Iijima, N. Nimura, M. Sigematsu, T. Tazawa, S. Mutsumoto, K. Kojima, and Y. Nagasawa, *Handbook of and X-ray Photoelectron Spectroscopy*. Tokyo, Japan: JEOL, 1991.
26. Childs, Kenton D., et. al. *Handbook of Auger Electron Spectroscopy*. USA.: Physical Electronics, 1995.



สถาบันวิทยบริการ
วไลยอลงกรณ์มหาวิทยาลัย



สถาบันวิทยบริการ
วไลยอลงกรณ์มหาวิทยาลัย

APPENDIX I

PRINCIPLE OF X-RAY PHOTOELECTRON SPECTROSCOPY AND AUGER ELECTRON SPECTROSCOPY

A1.1 X-ray Photoelectron Spectroscopy

X-ray photoelectron spectroscopy (XPS) is a surface analysis method based on photoelectric effect as exemplified in Figure A.1. In this method the incident x-ray with the energy of $h\nu$, where h is a plank constant and ν is a frequency of X-ray, impinges on surface and causes the creation of the inner shell vacancy. To release the electron in that shell from surface, which is called photoelectron, the primary energy of X-ray must be equal or more than the sum of binding energy of electron in that level, E_b , and work function, ϕ . The remaining energy between the energy of primary X-ray and the sum of binding energy of electron in that level and work function is kinetic energy of photoelectron, K.E., according to the following equation.(24)

$$\text{K.E.} = h\nu - (E_b + \phi) \dots\dots\dots \text{A1.1}$$

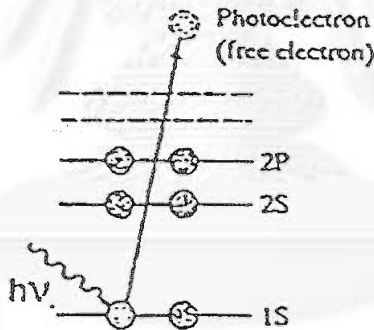


Figure A.1 Schematic diagram of photoelectric effect excited by primary X-ray (25)

In XPS experiment, according to equation A1.1, kinetic energy of emitted photoelectron is detected, the energy of primary X-ray, $h\nu$, is known depending on X-ray source used. By estimating work function, binding energy is then obtained. The binding energy is unique for any element and the analytical depth is in the order of nanometer. The detection of kinetic energy of photoelectron and therefore binding energy of photoelectron is then applied to investigate the existence of elements in surface film. Furthermore, because binding energy changes with the change of chemical state of element, XPS then can be applied not only a kind of element, but also the different chemical states in each element.

To identify photoelectron, the notation such as $\text{Fe}2p_{3/2}$ is determined. Fe indicate element in consideration. The shell and orbital that electron of that element is in are characterized by 2 and p respectively. $3/2$ is carried out from the vectorial summation of the quantum number of orbital angular momenta, l , and of spin momenta, s . In this case, l is 1 and s is $1/2$.

The primary information of this technique is the integrated peak intensity depicted as raw area constraint by a certain range of binding energy and bounded by intensity line and background line. Such area can be quantified to obtain the numerical value of photoelectron intensity. By using the quantification method, such as that will be explained in appendix II, atomic, and therefore mass percent, can be obtained.

A1.2 Principle of Auger Electron Spectroscopy

Auger electron spectroscopy (AES) is a surface analysis method based on Auger effect as exemplified in Figure A.2. In this method the incident electron impinges on surface and causes the creation of the inner shell vacancy, which is in K level in this Figure. To relax this excitation, electron in the outer level, which is L_{II} in this case, drops to the inner vacancy causing the radiation of the energy equal to the difference between the binding energy of electron in K level and L_{II} level denoted as $E_K - E_{LII}$. This energy transfers to another electron, which is in L_{III} level in this case. Energy required to release the latest electron, which is called as Auger electron, from surface is equal to the sum of binding energy of electron in that level, which is in L_{III} level denoted as E_{LIII} in this Figure, and work function denoted as ϕ . Kinetic energy of the Auger electron is then as follows (26)

$$KE_{KLIII} = (E_K - E_{LII}) - (E_{LIII} + \phi) \dots \dots \dots A1.2$$

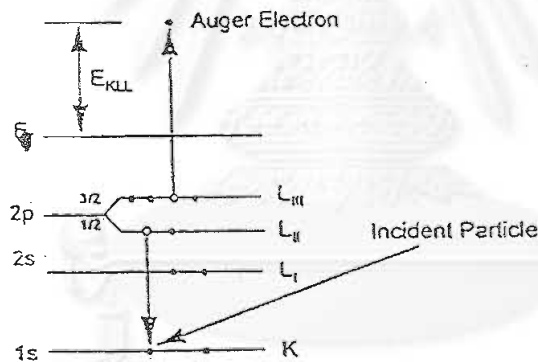


Figure A12 Schematic diagram of Auger process excited by primary electron (26)

KE_{KLIII} means kinetic energy of Auger electron that causes by the creation of initial vacancy in K level and the excitation is relaxed by the filling of electron from L_I level to K level and by the emitting of Auger electron from L_{III} level with kinetic energy corresponding to equation A.1. It may be written simply as KE_{KLL} .

Because the detected kinetic energy of Auger electron is unique for any element and the analytical depth is in the order of nanometer, the detection of this energy is then applied to investigate the existence of elements in surface film. By detecting Auger electron emitted from surface with the sputtering of surface alternately or simultaneously. Depth profile then can be obtained. This mode of AES application benefits to investigate elemental distribution in surface film and to estimate the surface film thickness. The detection of Auger electron with the sputtering passive film alternately was applied in the present work in order to estimate passive film thickness.

APPENDIX II

XPS QUANTIFICATION BY RELATIVE SENSITIVITY FACTOR

Relative sensitivity factor (RSF) is purposed to transform photoelectron intensity to atomic concentration. It is a conventional method that is still used in an industrial research such as in Kawasaki Steel Corporation.

In an alloy consists of n elements and photoelectron intensities are I_1, I_2, \dots, I_n count/second, atomic concentration of element j is derived as follows.

$$\%X_j = (I_j/RSF_j) / \sum (I_i/RSF_i) \dots\dots\dots A.2.1$$

RSF_j is relative sensitivity factor of element i . The term of $\sum (I_i/RSF_i)$ is summed for n elements. To obtain RSF and accuracy of a measurement practically, standard specimens with the given chemical compositions are applied in XPS analysis.

For instance, to obtain RSF of each element and the accuracy of experiment, equation A2.1 is manipulated as follows;

$$\sum (I_i/RSF_i) = (I_j/RSF_j) / \%X_j = (I_k/RSF_k) / \%X_k \dots\dots\dots A.2.2$$

whereas j and k are indices for element j and k respectively. By setting $RSF_j=1$, the following relation can be drawn.

$$(\%X_j/\%X_k) = RSF_k(I_j/I_k) \dots\dots\dots A2.3$$

$$RSF_k = (\%X_j/\%X_k)/(I_k/I_j) \dots\dots\dots A2.4$$

From equation A2.3, it can be seen that quantification by this method based on the assumption of the direct proportion of relative photoelectron intensity and relative atomic concentration of arbitrary two elements in a system. From equation A2.4, because atomic concentration can be known from standard specimens and photoelectron intensities are obtained by experiment, then RSF_k can be obtained according to equation A2.4. RSF for other elements can be derived in the same way. However, if experiments were carried out to detect photoelectron in m standard specimens. Average RSF for each element can be finally obtained by averaging RSF obtained from each standard specimen.

To evaluate the accuracy of a measurement, the average RSF finally obtained is applied in equation A2.4 with the detected photoelectron intensities. The calculated atomic concentration is then obtained, and can be change to mass concentration. The accuracy, σ_d , is defined as follows.

$$\sigma_d = \{ \sum (\%C_{cal.} - \%C_{std.})^2 / (m-1) \}^{1/2} \dots\dots\dots A2.5$$

$\%C_{cal.}$ is calculated mass concentration by using RSF, $\%C_{std.}$ is standard mass concentration given by standard specimens. The term of $\sum (\%C_{cal.} - \%C_{std.})^2$ is summed for m standard specimens. Relative sensitivity factors and accuracy of XPS measurement in the present work were investigated in appendix III.

APPENDIX III

EXPERIMENT FOR INVESTIGATING THE ACCURACY OF XPS QUANTIFICATION BY USING RSF METHOD

A3.1 Objectives

To obtain relative sensitivity factors (RSFs) of Fe, Cr and Ni accompanied by the accuracy of XPS experiment for stainless steels.

A3.2 Scope

RSF is estimated from bulk part of standard stainless steel.

A3.3 Experimental method

A3.3.1 Specimens

JSS 650-13, JSS651-13, JSS652-13, JSS653-13, JSS654-13 and JSS655-13 are standard stainless steels used. Chemical compositions of them are tabled in Table 1. They were cut to be the cross section of 10mm x 10mm. The ultrasound cleaning and degreasing by acetone was applied before analysis.

Table A3.1 Mass percent of standard stainless steels used

Steel(JS S)	Mass%										
	C	Si	Mn	P	S	Ni	Cr	Mo	Cu	Co	Nb
650-13	0.053	0.3	0.48	0.024	-	0.18	16.7	0.013	0.02	0.017	-
651-13	0.018	0.42	1.81	0.026	0.003	10.2	18.42	0.24	0.16	0.13	-
652-13	0.044	0.42	1.73	0.031	0.003	11.38	16.56	2.13	0.2	0.18	-
653-13	0.044	0.4	1.8	0.033	0.0006	13.96	22.43	0.2	0.16	0.2	-
654-13	0.04	0.4	1.69	0.026	0.0006	19.42	24.79	0.23	0.15	0.15	-
655-13	0.036	0.62	1.81	0.028	0.004	9.52	17.34	0.22	0.2	0.17	0.55

A3.3.2 XPS analysis

The instrument was performed with KRATOS AXIS HS. AlK α monochromatic x-ray contained the photon energy of 1486.6 eV was applied with the x-ray power of 15 kVx5mA. The incident angle of X-ray was 55° to the surface normal, whereas the take-off angle was 90°. The pass energy of 40 eV was used. The energy axis was horizontal shifted to set the binding energy of C1s at 284.6 eV. Linear base line was drawn in order to quantify integrated peak intensity.

A3.4 Results

Raw area of photoelectron intensity of Fe, Cr and Ni was tabled in Table A3.2. And according to the derivation of relative sensitivity factors (RSFs) and accuracy of measurement explained in appendix 2, those values were calculated and tabled in Table A3.3.

Table A3.2 Raw area obtained from standard stainless steels

Steel(JSS)	Fe	Cr	Ni
650-13	13463	2571	0
651-13	18436	4585	2962
652-13	13529	2971	2413
653-13	17858	6238	4333
654-13	14731	6649	5676
655-13	20914	4670	3246

Table A3.3 RSFs and % accuracy of a measurement

	Fe	Cr	Ni
RSF	1	0.86	1.13
%accuracy	2.5	0.85	0.52

A3.5 Conclusion

In XPS experiment for standard stainless steels, photoelectron emitted from the bulk parts was detected in order to find out the relative sensitivity factors accompanied by the accuracy of the experiments. The following conclusion can be drawn;

1. Relative sensitivity factors of Cr and Ni normalized by Fe are 0.86 and 1.13 respectively.
2. Accuracy of XPS measurement of Fe, Cr and Ni in bulk stainless steels are 2.5%, 0.85% and 0.52% respectively.

สถาบันวิทยบริการ
จุฬาลงกรณ์มหาวิทยาลัย

VITAE

NAME: Somrerk CHANDRA-AMBHORN

PERSONAL DATA: Birth date: Sept. 24th, 1977

Birthplace: Rachaburi Province, Thailand

Martial Status: Single

EDUCATION:

Grade 5-9: Bhumipol King's College,
Nakorn Pathom, Thailand, 1987-1992

Grade 10-12: Triam Udom Suksa School,
Bangkok, Thailand, 1992-1995

Undergraduate School: Chulalongkorn University,
Bangkok, Thailand, 1995-1999
B.Eng. (Metallurgical Engineering)

Graduate School: Chulalongkorn University,
Bangkok, Thailand, 1999-2001
M.Eng. (Metallurgical Engineering)
(Expected to be held in October 2001)

WORK EXPERIENCES :

November 1999 to
March 2000 Teaching Assistant,
Heat treatment laboratory,
Chulalongkorn University, Bangkok, Thailand

October 2000 to
April 2001 Co-operative Research Student,
Kawasaki Steel Corporation, Chiba, Japan

PUBLICATIONS:

1. S. Chandra-ambhorn, P. Leejinda, E. Viyanit and G. Lothongkum,
"Acceptable TIG Pulse Welding Parameters of 316L Austenitic Stainless Steel at 8
and 10 h Welding Positions", *Proceedings on the First Thailand Materials Science
and Technology Conference*, Bangkok, Thailand, 2000, pp.44-46.